

NAVAL POSTGRADUATE SCHOOL Monterey, California

AD-A202 192



DTIC FILE COPY

THESIS

DTIC
ELECTE
S JAN 3 1989 D
& H

FINITE ELEMENT ANALYSIS OF
LAMINATED COMPOSITE PLATES

by

Lee, Myung-Ha

September 1988

Thesis Advisor:

Dr. Ramesh Kolar

Approved for public release; distribution is unlimited

89 1 03 031

REPORT DOCUMENTATION PAGE

1a REPORT SECURITY CLASSIFICATION Unclassified		1b RESTRICTIVE MARKINGS	
2a SECURITY CLASSIFICATION AUTHORITY		3 DISTRIBUTION/AVAILABILITY OF REPORT Approved for public release; distribution is unlimited	
2b DECLASSIFICATION/DOWNGRADING SCHEDULE		5 MONITORING ORGANIZATION REPORT NUMBER(S)	
4 PERFORMING ORGANIZATION REPORT NUMBER(S)		7a NAME OF MONITORING ORGANIZATION Naval Postgraduate School	
6a NAME OF PERFORMING ORGANIZATION Naval Postgraduate School	6b OFFICE SYMBOL (if applicable) Code 67	7b ADDRESS (City, State and ZIP Code) Monterey, California 93943-5000	
8a NAME OF FUNDING SPONSORING ORGANIZATION		9 PROCUREMENT INSTRUMENT IDENTIFICATION NUMBER	
8b ADDRESS (City, State and ZIP Code)		10 SOURCE OF FUNDING NUMBERS	
		PROGRAM ELEMENT NO	PROJECT NO
		TASK NO	WORK UNIT ACCESSION NO
11 TITLE (include Security Classification) FINITE ELEMENT ANALYSIS OF LAMINATED COMPOSITE PLATES			
12 PERSONAL AUTHOR(S) Lee, Myung-Ha			
13a TYPE OF REPORT Master's Thesis	13b TIME COVERED FROM TO	14 DATE OF REPORT (Year, Month, Day) 1988, September	15 PAGE COUNT 73
16 SUPPLEMENTARY NOTES The views expressed in this thesis are those of the author and do not reflect the official policy or position of the Department of Defense or the U.S. Government.			
17 COSAT CODES		18 SUBJECT TERMS (Continue on reverse if necessary and identify by block number)	
FIELD	GROUP	Finite Element, Plate/Shell Bending, Laminated Composites	
19 ABSTRACT (Continue on reverse if necessary and identify by block number)			
<p>A biquadratic isoparametric plate/shell bending finite element is developed to study the behavior of isotropic and laminated composite plates. The element is based on Mindlin-Reissner's theory and the principle of virtual displacements. The element is implemented in a computer program. Results are presented and compared with analytical solutions to validate this element. Good agreement is observed for thin plates, while discrepancies are noted for thick plates. Effects of various integration schemes on the element performance are presented. Convergence studies for laminated composites for different fiber orientations are also discussed.</p> <p>Keywords: Composite Structures, Flat Plate, Structural Mechanics, Strain Mechanics, Displacement, Graphical Quadrature, Graphite, Epoxy Composites, Glass, Shell Plates, Deformation, Thesis. (A1)</p>			
20 DISTRIBUTION/AVAILABILITY OF ABSTRACT <input checked="" type="checkbox"/> UNCLASSIFIED/UNLIMITED <input type="checkbox"/> SAME AS RPT <input type="checkbox"/> DTIC USERS		21 ABSTRACT SECURITY CLASSIFICATION Unclassified	
22a NAME OF RESPONSIBLE INDIVIDUAL Professor Ramesh Kolar		22b TELEPHONE (include Area Code) (408) 640-2936	22c OFFICE SYMBOL Code 67K1

Approved for public release; distribution is unlimited

Finite Element Analysis of Laminated Composite Plates

by

Myung-Ha Lee
Major, Korea Air Force
B.S., Korea Air Force Academy, 1979

Submitted in partial fulfillment of the
requirements for the degree of

MASTER OF SCIENCE
IN AERONAUTICAL ENGINEERING

from the

NAVAL POSTGRADUATE SCHOOL

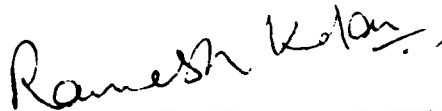
September 1988

Author:



Myung-Ha Lee

Approved by:



Ramesh Kolar. Thesis Advisor



E. Roberts Wood, Chairman
Department of Aeronautics and Astronautics



Gordon E. Schacher
Dean of Science and Engineering

ABSTRACT

A bi-quadratic isoparametric plate/shell bending finite element is developed to study the behavior of isotropic and laminated composite plates. The element is based on Mindlin-Reissner's theory and the principle of virtual displacements. The element is implemented in a computer program. Results are presented and compared with analytical solutions to validate this element. Good agreement is observed for thin plates, while discrepancies are noted for thick plates. Effects of various integration schemes on the element performance are presented. Convergence studies for laminated composites for different fiber orientations are also discussed.



Accession For	
NTIS GRA&I	<input checked="" type="checkbox"/>
DTIC TAB	<input type="checkbox"/>
Unannounced	<input type="checkbox"/>
Justification	
By	
Distribution/	
Availability Codes	
Dist	Avail and/or Special
A-1	

TABLE OF CONTENTS

I.	INTRODUCTION	1
	A. THE SCOPE OF THE THESIS	1
	B. LITERATURE SURVEY	2
II.	THEORETICAL FORMULATION	4
	A. INTRODUCTION	4
	B. THE PRINCIPLE OF VIRTUAL WORK	4
	C. LAMINATE THEORY	8
	1. <u>Introduction</u>	8
	2. <u>Strain-displacement Relations</u>	8
	3. <u>Stress-Strain Relations</u>	9
	4. <u>Lamina of Composite Materials</u>	11
	5. <u>Laminate Analysis</u>	15
	D. $[B]$, THE STRAIN-DISPLACEMENT MATRIX	18
	1. <u>Introduction</u>	18
	2. <u>Shape Functions and Their Derivatives</u>	18
	3. <u>Jacobian Transformation Matrix</u>	22
	4. <u>Formation of $[B]$ Matrix</u>	26
	E. GAUSSIAN QUADRATURE	27
	1. <u>Introduction</u>	27
	2. <u>Summary of Gauss Quadrature</u>	27
III.	PROGRAM IMPLEMENTATION	31
	A. INTRODUCTION	31
	B. SOLUTION PROCEDURE	31

IV.	NUMERICAL EXAMPLES	35
A.	INTRODUCTION	35
B.	SIMPLY SUPPORTED SQUARE ISOTROPIC PLATE	35
	1. <u>Simply supported plate under concentrated load.</u>	35
	2. <u>Simply Supported Plate under Distributed Load</u>	37
C.	CLAMPED-CLAMPED SQUARE ISOTROPIC PLATE	37
D.	CANTILEVERED ISOTROPIC PLATE	44
E.	SIMPLY SUPPORTED LAMINATED PLATE	44
	1. <u>Graphite-epoxy</u>	44
	2. <u>Glass-Epoxy</u>	49
V.	CONCLUSIONS	57
	LIST OF REFERENCES	58
	INITIAL DISTRIBUTION LIST	61

LIST OF TABLES

2.1	Shape Function and Their Derivatives	24
2.2	Coefficients for Gaussian Quadrature	30

LIST OF FIGURES

2.1 Displacement and Distortion of Differential Lengths dx and dy	10
2.2 Lamina Coordinate System (2-Dimension)	12
2.3 Positive Directions for Stress Resultants and Stress Couples for a Lamina	19
2.4 Lagrangian Plate Element	21
2.5 Degrees of Freedom at a Typical Node i	22
2.6 Displacements in the x - z Plane	23
2.7 Gaussian Quadrature (ξ Coordinate) using Three Sampling Points	29
3.1 Flow Chart (Main Program)	32
3.2 Flow Chart (KQML9)	34
4.1 A Rectangular Isotropic Plate under Concentrated Point Load	36
4.2 W/W_{anal} vs. $\text{Log}(L/T)$ on Simply Supported Square Plate under Central Point Load.	38
4.3 W/W_{anal} vs. No. of Elements on Simply Supported Square Plate under Central Point Load.	39
4.4 A Rectangular Isotropic Plate under Distributed Load	40
4.5 $W/W_{(anal)}$ vs. No. of Elements on Simply Supported Plate Under Distributed Load	41
4.6 $W/W_{(anal)}$ vs. $\text{Log}(L/T)$ on Simply Supported Plate Under Dis- tributed Load	42
4.7 A Clamped-Clamped Rectangular Plate Under Distributed Load	43
4.8 $W/W_{(anal)}$ vs. $\text{Log}(L/T)$ for Clamped-Clamped Plate under Dis- tributed Load	45

4.9	Nondimensional Deflection vs. No. of Element for Clamped-Clamped Plate under Distributed Load	46
4.10	Cantilevered Plate	47
4.11	$W/W_{(anal)}$ vs. No. of Element for Cantilevered Plate	48
4.12	Central Deflection W_{max} of 4-Layered Square Plate	50
4.13	W_{max} vs. No. of Elements for 4-Layered Square Plate	51
4.14	W_{max} vs. No. of Elements for 4-Layered Square Plate	52
4.15	Central Deflection W_{max} for 4-Layered Square Plate	54
4.16	W_{max} vs. No. of Elements for 4-Layered Square Plate	55
4.17	W_{max} vs. No. of Elements for 4-Layered Square Plate	56

ACKNOWLEDGMENT

A bi-quadratic isoparametric plate/shell bending finite element is developed to study the behavior of isotropic and laminated composite plates. The element is based on Mindlin-Reissner's theory and the principle of virtual displacements. The element is implemented in a computer program. Results are presented and compared with analytical solutions to validate this element. Good agreement is observed for thin plates, while discrepancies are noted for thick plates. Effects of various integration schemes on the element performance are presented. Convergence studies for laminated composites for different fiber orientations are also discussed.

I. INTRODUCTION

A. THE SCOPE OF THE THESIS

Finite element analysis provides a general tool to solve problems in structural mechanics. The methodology is applicable for static and dynamic response of structures and in predicting the elastic stability limits.

The focus of the present study is to develop tools to analyze laminated composite plates and validate the model by comparing with known solutions.

More specifically, the objectives of the present study are:

- a) to review some of the pertinent literature in the area of laminated composite plates.
- b) develop a finite element for the analysis of composite plates.
- c) develop consistent mass and load matrices.
- d) study the effect of thickness to characteristic length of the plate.
- e) study the effects of integration schemes.

The outline of the remainder of this thesis is as follows:

The basic formulation of the stiffness, mass and load matrix for the bending of flat plates using laminated composite materials are described in Chapter II.

Chapter III addresses certain aspects of computational implementation.

Chapter IV describes some test cases, example calculations and comparison with classical plate theory.

Finally, Chapter V reflects experience gained and some suggestions for future research.

B. LITERATURE SURVEY

The finite element method, [Ref. 1], may be described as a general discretization procedure of continuum problems, posed by mathematically defined statements with applications to several engineering analysis problems.

A brief literature review pertaining to the analysis of plates/shells using finite element approximation is presented in the following paragraphs. A significant contribution to include shear is given by Mindlin [Ref. 2], while Hughes et al, [Ref. 3] adapt this theory to develop finite elements for the analysis of isotropic plates [Refs. 3, 4]. Laminated plate theory based on the classical Kirchoff hypothesis has been established by Reissner and Starsky [Ref. 5] and Whitney and Leissa [Ref. 6]. The effect of reduced integration in isoparametric elements was presented by Zienkiewicz et al [Ref. 7] and Hughes et al [Ref. 3].

The finite element method of analysis for the plate bending problem including shear deformation has been presented by Pryor and Barker [Ref. 8]. Mawenya describes formulations for multi-layer plates [Refs. 9, 10]. The higher order shear deformation theory of laminated composite plates was developed by Krishna Murty [Ref. 11], and Lo et.al. [Refs. 12, 13] present a higher order, three-dimensional theory.

Burt [Ref. 14] presented a higher order theory and compared with Pagano's elasticity-theory solution for the case of cylindrical bending and a symmetric cross-ply laminate consisting of three equal-thickness layers. Bending of simply supported thick rectangular plates was presented by Srinivas and Rao [Ref. 15]. Exact elasticity solutions for some particular plate bending problems have been obtained by Pagano [Refs. 16, 17, 18, 19] and Srinivas and Rao [Ref. 20].

Application of classical shell theory, including transverse shear deformation is presented by Vinson and Chou [Ref. 21]. Naschie [Ref. 22] studied large deflection behavior of orthotropic composite materials. Srinivas [Ref. 23] developed a refined approximate theory for the static and dynamic analysis of finite, laminated, composite, circular cylindrical shells with general boundary conditions.

Plate theories, which include shear deformation has been developed by Whitney [Ref. 24] and Mau [Ref. 25]. The first such theory for laminated isotropic plates is due to Yang, Norris and Stravinsky [Ref. 26]. Reddy [Ref. 27] developed a higher order shear deformation theory of laminated composite plates. Reddy and Sandidge [Ref. 28] presented mixed finite element models of the classical and shear deformation theory. The effect of transverse shear deformation on bending of elastic symmetric laminated composite plate undergoing large deformation is presented by Gorji [Ref. 29].

Based on anisotropic elasticity, Hearmon [Ref. 30] and Lekhnitskii [Ref. 31] present general theories for laminates. The covariant form for the transformed lamina stiffnesses has been given by Tsai and Pagano [Ref. 33]. Gibert and Schneider [Ref. 34] directed their study in this direction. Noor and Mathers [Refs. 35, 36] presented the effects of shear deformation and anisotropy on the response of laminated anisotropic plates.

Nelson and Lorch [Ref. 40] compare the accuracy of various plate models to predict the behavior of laminated orthotropic plates.

II. THEORETICAL FORMULATION

A. INTRODUCTION

In this chapter, the derivation of plate finite elements based on Mindlin's theory is described. The principle of virtual displacements is invoked to obtain equilibrium relations.

B. THE PRINCIPLE OF VIRTUAL WORK

In this section, we prove that total internal virtual work is equal to total external virtual work and equivalence of this principle to the minimum total potential energy principle.

In general, the total potential energy of a structural system is equal to the sum of strain energy and potential energy.

$$\Pi_p = U + V \quad (2.1)$$

where,

Π_p : Total Potential Energy of Structural System

U : Total Strain Energy

V : Total Potential of External Loads

The total minimum potential energy requires that first variation of total potential energy be zero, or

$$\delta\Pi_p = 0 \quad (2.2)$$

or,

$$\delta U + \delta V = 0 \quad (2.3)$$

in other words,

$$\delta U = -\delta V \quad (2.4)$$

This may also be written in a different form, recognizing U as being the work done by internal forces and that work done by the external forces being equal to the negative of the total potential energy of the external loads. That is,

$$\delta W_{int} = \delta W_{ext} \quad (2.5)$$

which is a statement of the principle of virtual work, stating that, if the body is in equilibrium, the total virtual work done by the internal forces is equal to the total virtual work done by external forces for arbitrary, kinematically admissible virtual displacements.

It may be noted that the form in Equation (2.4) is restricted to conservative loadings while the form in Equation (2.5) is applicable for any loading form.

The total internal virtual work may be written as

$$\delta W_{int} = \int_{vol} \{\sigma\}^T \{\delta\epsilon\} d(A) \quad (2.6)$$

where,

$\{\sigma\}$: Vector of Stresses
 $\{\delta\epsilon\}$: Vector of Virtual Strains

By using generalized Hooke's law for material constitutive relations, stresses may be expressed as

$$\{\sigma\} = [Q]\{\epsilon\} \quad (2.7)$$

where the matrix $[Q]$ contains the material stiffness coefficients.

If the thickness t is constant, then total internal virtual work takes the form,

$$\delta W_{int} = \int_A t\{\epsilon\}^T [Q] \{\delta\epsilon\} d(vol) \quad (2.8)$$

In order to derive the element matrices, the principle of virtual work, which is equally applicable to the element as well as to the total structure, is applied to the element. The virtual work is additive and results in the virtual work of the entire structure under consideration.

The linear strain-displacement relations are given by

$$\{\epsilon\} = [B]\{u\} \quad (2.9)$$

while the virtual strains are given by

$$\{\delta\epsilon\} = [B] \{\delta u\} \quad (2.10)$$

The operator matrix, $[B]$, is dependent on the shape functions and their derivatives, and $\{u\}$ and $\{\delta u\}$ are vectors of displacements and virtual displacements, respectively of the element.

On substituting Equation (2.9), (2.10) in Equation (2.8), we obtain,

$$\delta W_{int} = \int_A t(\{\delta u\}^T [B]^T)[Q]([B]\{\delta u\})dA \quad (2.11)$$

or, rearranging

$$\delta W_{int} = \{\delta u\}^T (t \int_A [B]^T [Q] [B] dA) \quad (2.12)$$

$$\delta W_{int} = \{\delta u\}^T [K] \quad (2.13)$$

where $[K] = t \int_A [B]^T [Q] [B] dA$ is the element stiffness matrix.

In order to derive mass and load matrices, we start from the expression for external virtual work,

$$\delta W_{ext} = \int \bar{T}\{\delta u\}ds - \int x\{\delta u\}d(vol) + \{\delta u\}^T\{F\} \quad (2.14)$$

where, \bar{T} is the external force per unit length along the boundary of the element,
 x is the body force per unit volume (inertia force)
 $\{F\}$ is the point loads applied at nodal points.

On substituting for displacements in terms of nodal displacements using shape functions, we obtain,

$$\delta W_{ext} = \{\delta u\}^T \left(\int_s [N]\bar{T}ds \right) - \{\delta u\}^T \left(\int_A t\rho[N][N]^T dA \right) [u] + \{\delta u\}^T \{F\} \quad (2.15)$$

By invoking the principle of virtual displacements and noting that $\{\delta u\}$ is arbitrary, we get the equilibrium equations in the following form;

$$[K]\{u\} + [M]\{u\} = [F] + [F]^d \quad (2.16)$$

where,

$$[M] = \int_A t\rho[N][N]^T dA \quad (2.17)$$

$$[F] = \begin{Bmatrix} F_1 \\ \vdots \\ F_n \end{Bmatrix} \quad (2.18)$$

$$[F]^d = \int_s [N]\bar{T}ds \quad (2.19)$$

It may be noted that the matrix $[M]$ is the mass matrix, $[F]$ is the vector of point loads and $[F]^d$ is the vector of consistent loads.

C. LAMINATE THEORY

1. Introduction

In the expression for $[K]$ matrix, there are three unknown matrices. In this section, we discuss about calculation of $[Q]$ matrix. The matrix $[Q]$, relating stresses and strains, consists of material stiffness coefficients. It reflects the properties of both fibers and matrix.

The behavior of laminated plates is characterized by possible coupling between membrane action and bending action.

Following discussions review some aspects of the laminate theory.

2. Strain-displacement Relations

As shown in Figure 2.1, a general strain field converts configuration 012 to 0'1'2'.

Linearized normal strains may be written as:

$$\epsilon_x = \frac{\partial u}{\partial x} \quad (2.20)$$

and

$$\epsilon_y = \frac{\partial v}{\partial y} \quad (2.21)$$

The shear strain is defined as the amount of change in a right angle. For small angles,

$$\gamma_{xy} = \beta_1 + \beta_2 \quad (2.22)$$

$$= \frac{\partial u}{\partial y} + \frac{\partial v}{\partial x} \quad (2.23)$$

Similar expressions may be derived for other strain components.

The foregoing strain-displacement relations can be summarized in a matrix-operator form.

$$\begin{Bmatrix} \epsilon_x \\ \epsilon_y \\ \epsilon_z \\ \gamma_{xy} \\ \gamma_{yz} \\ \gamma_{zx} \end{Bmatrix} = \begin{bmatrix} \frac{\partial}{\partial x} & 0 & 0 \\ 0 & \frac{\partial}{\partial y} & 0 \\ 0 & 0 & \frac{\partial}{\partial z} \\ \frac{\partial}{\partial y} & \frac{\partial}{\partial x} & 0 \\ 0 & \frac{\partial}{\partial z} & \frac{\partial}{\partial y} \\ \frac{\partial}{\partial z} & 0 & \frac{\partial}{\partial x} \end{bmatrix} \begin{Bmatrix} u \\ v \\ w \end{Bmatrix} \quad (2.24)$$

3. Stress-Strain Relations

The generalized Hooke's Law takes the form,

$$\{\sigma\} = [Q]\{\epsilon\} \quad (2.25)$$

where, the stress vector is given by

$$\{\sigma\} = \{\sigma_x \sigma_y \sigma_z \tau_{xy} \tau_{yz} \tau_{zx}\} \quad (2.26)$$

and the strain vector is given by

$$\{\epsilon\} = \{\epsilon_x \epsilon_y \epsilon_z \gamma_{xy} \gamma_{yz} \gamma_{zx}\} \quad (2.27)$$

The material stiffness matrix $[Q]$, contains nine independent coefficients.

An orthotropic material has only five independent elastic coefficients $-E_1, E_2, \nu_{12}, \nu_{21},$ and G_{12} .

More explicitly, Equation (2.25) may be written as

$$\begin{Bmatrix} \sigma_x \\ \sigma_y \\ \sigma_z \\ \tau_{xy} \\ \tau_{yz} \\ \tau_{zx} \end{Bmatrix} = \begin{bmatrix} Q_{11} & Q_{12} & Q_{13} & 0 & 0 & 0 \\ Q_{21} & Q_{22} & Q_{23} & 0 & 0 & 0 \\ Q_{31} & Q_{32} & Q_{33} & 0 & 0 & 0 \\ 0 & 0 & 0 & Q_{44} & 0 & 0 \\ 0 & 0 & 0 & 0 & Q_{55} & 0 \\ 0 & 0 & 0 & 0 & 0 & Q_{66} \end{bmatrix} \begin{Bmatrix} \epsilon_x \\ \epsilon_y \\ \epsilon_z \\ \gamma_{xy} \\ \gamma_{yz} \\ \gamma_{zx} \end{Bmatrix} \quad (2.28)$$

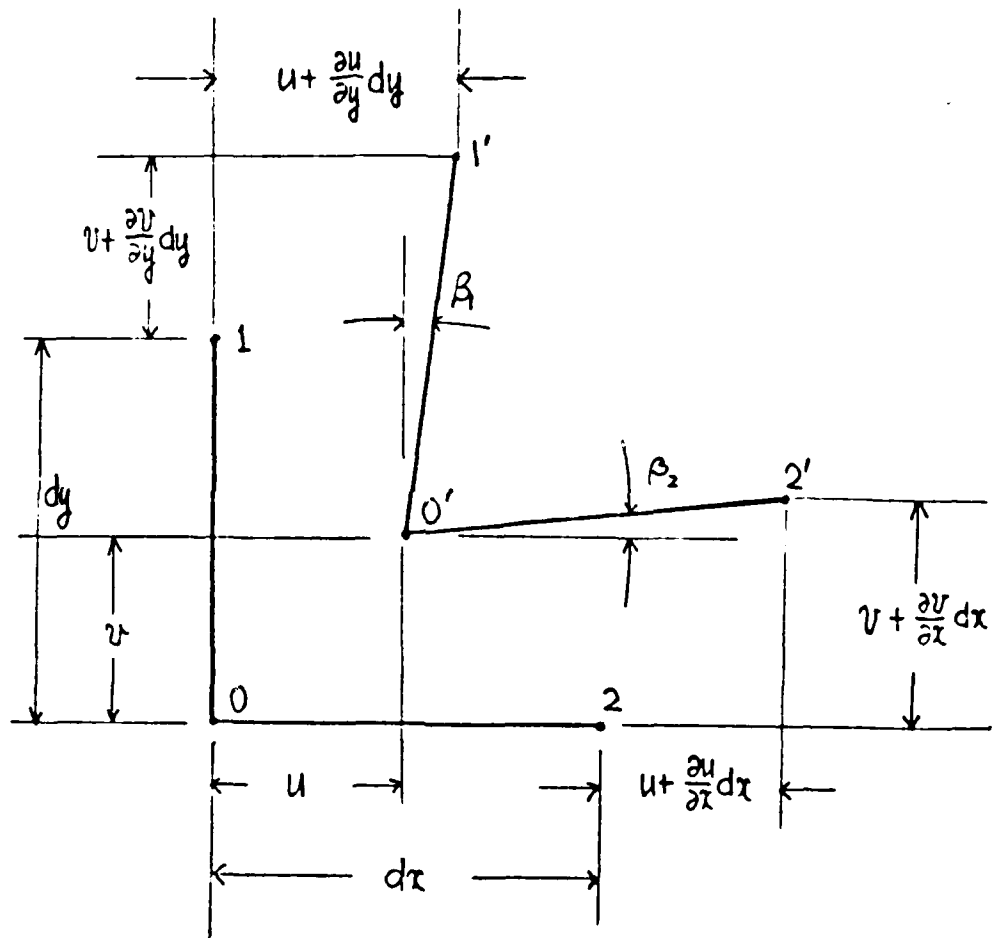


Figure 2.1: Displacement and Distortion of Differential Lengths dx and dy .

For planar orthotropic material, the stress-strain relation reduces to:

$$\begin{Bmatrix} \sigma_x \\ \sigma_y \\ \tau_{xy} \\ \tau_{yz} \\ \tau_{zx} \end{Bmatrix} = \begin{bmatrix} Q_{11} & Q_{12} & 0 & 0 & 0 \\ Q_{21} & Q_{22} & 0 & 0 & 0 \\ 0 & 0 & Q_{44} & 0 & 0 \\ 0 & 0 & 0 & Q_{55} & 0 \\ 0 & 0 & 0 & 0 & Q_{66} \end{bmatrix} \begin{Bmatrix} \epsilon_x \\ \epsilon_y \\ \gamma_{xy} \\ \gamma_{yz} \\ \gamma_{zx} \end{Bmatrix} \quad (2.29)$$

where,

$$Q_{11} = \frac{E_1}{1 - \nu_{12} \nu_{21}} \quad (2.30)$$

$$Q_{22} = \frac{E_2}{1 - \nu_{12} \nu_{21}} \quad (2.31)$$

$$Q_{44} = G_{12} \quad (2.32)$$

$$Q_{55} = G_{23} \quad (2.33)$$

$$Q_{66} = G_{13} \quad (2.34)$$

It may be noted that shears τ_{yz} and τ_{zx} are obtained to account for transverse shears.

4. Lamina of Composite Materials

Composite structures are built of individual lamina, which are stacked into several number of layers to form a laminate. Each lamina consists of, typically, uniaxial fibers embedded in a matrix, such as a resin. In Figure 2.2, the principal material axes are labelled 1 and 2, that is, 1-direction is parallel to the fibers direction and the 2-direction is normal to them.

It may be noted that in each lamina there exists a state of plane stress.

The state of stress is also shown in the Figure 2.2, in both 1-2 and x-y coordinate system. The computation stresses in different coordinate system follows the usual transformation rules [Ref. 21]. We follow the notation that σ_1, σ_2 are

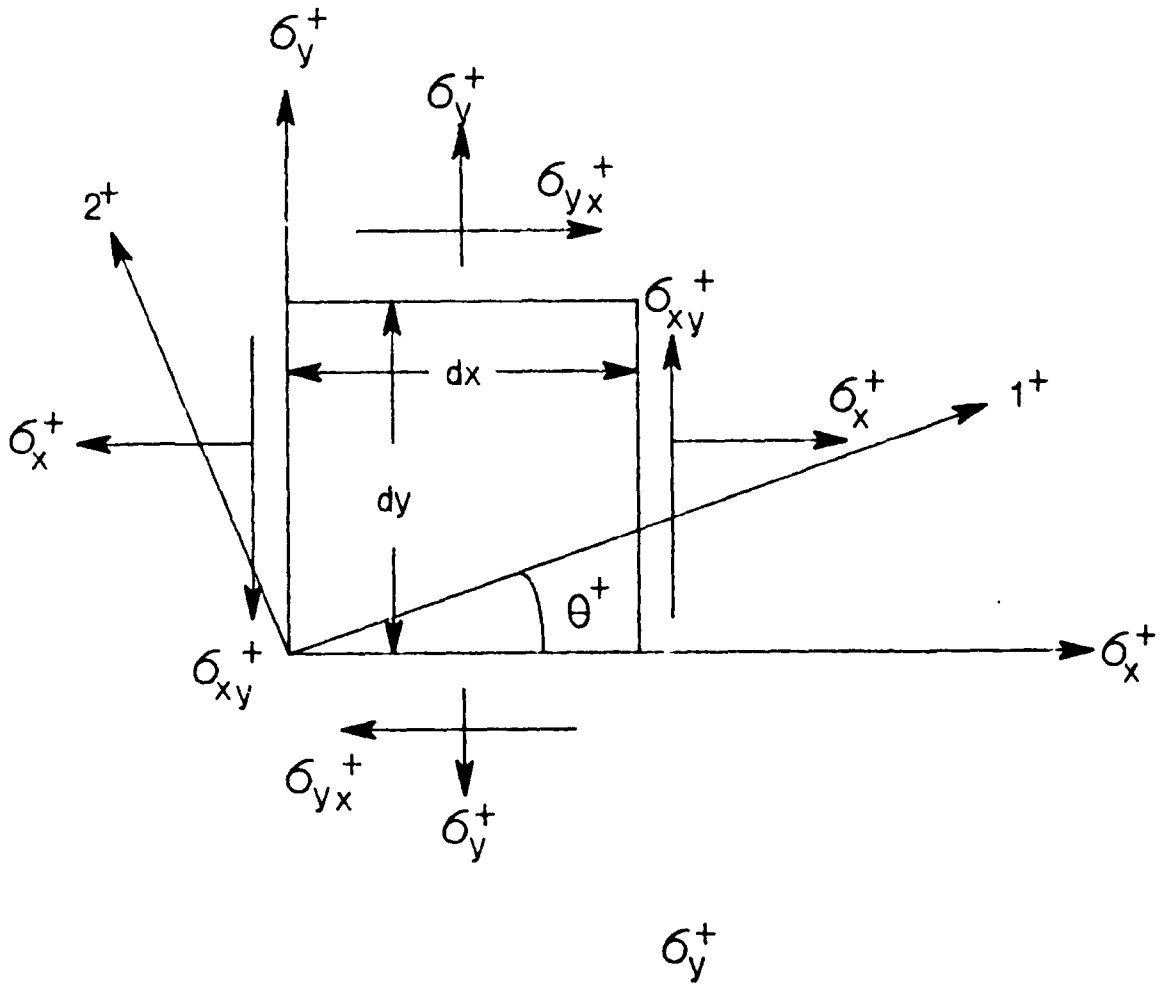


Figure 2.2: Lamina Coordinate System (2-Dimension)

normal stresses, σ_3, σ_4 and σ_5 are the shear stress in 1-2 system. $\epsilon_1, \epsilon_2, \epsilon_3, \epsilon_4$ and ϵ_5 are the corresponding strains in 1-2 system.

$$\begin{bmatrix} \sigma_1 \\ \sigma_2 \\ \sigma_4 \end{bmatrix} = [T]_{CL} \begin{bmatrix} \sigma_x \\ \sigma_y \\ \tau_{xy} \end{bmatrix} \quad (2.35)$$

where the transformation matrix is given by

$$[T]_{CL} = \begin{bmatrix} m^2 & n^2 & 2mn \\ n^2 & m^2 & -2mn \\ -mn & mn & (m^2 - n^2) \end{bmatrix} \quad (2.36)$$

The direction cosines of the unit normal are determined from

$$m = \cos \theta \quad (2.37)$$

$$n = \sin \theta \quad (2.38)$$

The subscript *CL* refers to two-dimensional case, that is the x-y plane only. Similarly, the strains are related in the two coordinate systems by

$$\begin{bmatrix} \epsilon_1 \\ \epsilon_2 \\ \epsilon_{12} \end{bmatrix} = [T]_{CL} \begin{bmatrix} \epsilon_x \\ \epsilon_y \\ \gamma_{xy} \end{bmatrix} \quad (2.39)$$

By including transverse shears, we modify these transformations as follows:

$$\begin{bmatrix} \sigma_1 \\ \sigma_2 \\ \sigma_3 \\ \sigma_4 \\ \sigma_5 \end{bmatrix} = [T] \begin{bmatrix} \sigma_x \\ \sigma_y \\ \tau_{xy} \\ \tau_{yz} \\ \tau_{zx} \end{bmatrix} \quad (2.40)$$

$$\begin{bmatrix} \epsilon_1 \\ \epsilon_2 \\ \epsilon_3 \\ \epsilon_4 \\ \epsilon_5 \end{bmatrix} = [T] \begin{bmatrix} \epsilon_x \\ \epsilon_y \\ \gamma_{xy} \\ \gamma_{yz} \\ \gamma_{zx} \end{bmatrix} \quad (2.41)$$

where the transformation is given by,

$$[T] = \begin{bmatrix} m^2 & n^2 & 2mn & 0 & 0 \\ n^2 & m^2 & -2mn & 0 & 0 \\ -mn & mn & m^2 - n^2 & 0 & 0 \\ 0 & 0 & 0 & m & -n \\ 0 & 0 & 0 & n & m \end{bmatrix} \quad (2.42)$$

The stresses and strains in x-y system may simply be obtained from 1-2 system by inverting the matrix $[T]$.

$$\begin{bmatrix} \sigma_x \\ \sigma_y \\ \tau_{xy} \\ \tau_{yz} \\ \tau_{zx} \end{bmatrix} = [T]^{-1} \begin{bmatrix} \sigma_1 \\ \sigma_2 \\ \sigma_3 \\ \sigma_4 \\ \sigma_5 \end{bmatrix} \quad (2.43)$$

and,

$$\begin{bmatrix} \epsilon_x \\ \epsilon_y \\ \gamma_{xy} \\ \gamma_{yz} \\ \gamma_{zx} \end{bmatrix} = [T]^{-1} \begin{bmatrix} \epsilon_1 \\ \epsilon_2 \\ \epsilon_3 \\ \epsilon_4 \\ \epsilon_5 \end{bmatrix} \quad (2.44)$$

with

$$[T]^{-1} = \begin{bmatrix} m^2 & n^2 & -2mn & 0 & 0 \\ n^2 & m^2 & 2mn & 0 & 0 \\ mn & -mn & m^2 - n^2 & 0 & 0 \\ 0 & 0 & 0 & m & n \\ 0 & 0 & 0 & -n & m \end{bmatrix} \quad (2.45)$$

The stress-strain relations, then, in x-y system assumes the following form,

$$\begin{Bmatrix} \sigma_x \\ \sigma_y \\ \tau_{xy} \\ \tau_{yz} \\ \tau_{zx} \end{Bmatrix} = \begin{bmatrix} \bar{Q}_{11} & \bar{Q}_{12} & \bar{Q}_{13} & 0 & 0 \\ \bar{Q}_{21} & \bar{Q}_{22} & \bar{Q}_{23} & 0 & 0 \\ \bar{Q}_{31} & \bar{Q}_{32} & \bar{Q}_{33} & 0 & 0 \\ 0 & 0 & 0 & \bar{Q}_{44} & 0 \\ 0 & 0 & 0 & 0 & \bar{Q}_{55} \end{bmatrix} \begin{Bmatrix} \epsilon_x \\ \epsilon_y \\ \gamma_{xy} \\ \gamma_{yz} \\ \gamma_{zx} \end{Bmatrix} \quad (2.46)$$

where,

$$[\bar{Q}] = [T]^{-1} [Q] [T] \quad (2.47)$$

5. Laminate Analysis

As discussed earlier, the laminae are stacked to obtain a laminate. In this section, the theory associated with the mechanics of laminates is described.

Consider a laminate composed of N lamina. For the k^{th} lamina of the laminate, Equation (2.46) can be written as follows:

$$\begin{Bmatrix} \sigma_x \\ \sigma_y \\ \tau_{xy} \\ \tau_{yz} \\ \tau_{zx} \end{Bmatrix}_K = [\bar{Q}]_K \begin{Bmatrix} \epsilon_x \\ \epsilon_y \\ \gamma_{xy} \\ \gamma_{yz} \\ \gamma_{zx} \end{Bmatrix}_K \quad (2.48)$$

where all matrices must have the subscript K due to orientation of the particular lamina with respect to the plate x-y coordinates.

The functional form of the displacement for a plate are given by:

$$u(x, y, z) = u_o(x, y) + z\bar{\alpha}(x, y) \quad (2.49)$$

$$v(x, y, z) = v_o(x, y) + z\bar{\beta}(x, y) \quad (2.50)$$

$$w(x, y) = w_o(x, y) \quad (2.51)$$

where u_o , v_o and w_o are middle surface in plane displacements, $\bar{\alpha}$ and $\bar{\beta}$ are related to the rotations.

Substituting Equation (2.49), (2.50) and (2.51) into the Equation (2.24)

results in:

$$\epsilon_x = \frac{\partial u_o}{\partial x} + z \frac{\partial \bar{\alpha}}{\partial x} \quad (2.52)$$

$$\epsilon_y = \frac{\partial v_o}{\partial y} + z \frac{\partial \bar{\beta}}{\partial y} \quad (2.53)$$

$$\epsilon_z = 0 \quad (2.54)$$

$$\epsilon_{xy} = \frac{1}{2} \left(\frac{\partial u_o}{\partial y} + \frac{\partial v_o}{\partial x} \right) \quad (2.55)$$

$$\epsilon_{yz} = \frac{1}{2} \left(\bar{\beta} + \frac{\partial w}{\partial y} \right) \quad (2.56)$$

$$\epsilon_{zx} = \frac{1}{2} \left(\bar{\alpha} + \frac{\partial w}{\partial x} \right) \quad (2.57)$$

The mid surface strains are given by the following relations:

$$\epsilon_{x_o} = \frac{\partial u_o}{\partial x} \quad (2.58)$$

$$\epsilon_{y_o} = \frac{\partial v_o}{\partial y} \quad (2.59)$$

$$\epsilon_{xy_o} = \frac{1}{2} \left(\frac{\partial u_o}{\partial y} + \frac{\partial v_o}{\partial x} \right) \quad (2.60)$$

The curvature terms, associated with transverse bending are written in the form,

$$\kappa_x = \frac{\partial \bar{\alpha}}{\partial x} \quad (2.61)$$

$$\kappa_y = \frac{\partial \bar{\beta}}{\partial y} \quad (2.62)$$

$$\kappa_{xy} = \frac{1}{2} \left(\frac{\partial \bar{\alpha}}{\partial y} + \frac{\partial \bar{\beta}}{\partial x} \right) \quad (2.63)$$

On substituting the strain-displacement relations into the stress-strain relations, we obtain stresses in terms of displacement components,

$$\begin{Bmatrix} \sigma_x \\ \sigma_y \\ \tau_{xy} \\ \tau_{yx} \\ \tau_{zx} \end{Bmatrix}_K = [\bar{Q}]_K \begin{Bmatrix} \epsilon_{x_0} + z\kappa_x \\ \epsilon_{y_0} + z\kappa_y \\ \gamma_{xy_0} + z\kappa_{xy} \\ \gamma_{yz} \\ \gamma_{zx} \end{Bmatrix}_K \quad (2.64)$$

For plate/shell type structures, we define stress resultants N_x , N_y , N_{xy} , Q_x , Q_y , M_x , M_y , and M_{xy} , as shown in Figure 2.3. For the k_{th} layer, we may write,

$$\begin{Bmatrix} N_x \\ N_y \\ N_{xy} \\ Q_x \\ Q_y \end{Bmatrix} = \int_{-t/2}^{t/2} \begin{Bmatrix} \sigma_x \\ \sigma_y \\ \sigma_{xy} \\ \sigma_{yz} \\ \sigma_{zx} \end{Bmatrix} dz \quad (2.65)$$

For a laminate composed of N -layers, the normal stress resultants are given by

$$\begin{bmatrix} N_x \\ N_y \\ N_{xy} \end{bmatrix} = \sum_{k=1}^N \int_{t_{k-1}}^{t_k} \begin{bmatrix} \sigma_x \\ \sigma_y \\ \sigma_{xy} \end{bmatrix} dz \quad (2.66)$$

or, in terms of strains, we have

$$\begin{bmatrix} N_x \\ N_y \\ N_{xy} \end{bmatrix} = \sum_{k=1}^N \left\{ \int_{t_{k-1}}^{t_k} [\bar{Q}]_K \begin{bmatrix} \epsilon_{x_0} \\ \epsilon_{y_0} \\ \epsilon_{xy_0} \end{bmatrix} dz + \int_{t_{k-1}}^{t_k} [\bar{Q}]_K \begin{bmatrix} \kappa_x \\ \kappa_y \\ \kappa_{xy} \end{bmatrix} z dz \right\} \quad (2.67)$$

The equation (2.67) may be written in the form

$$[N] = [A][\epsilon_0] + [B][\kappa] \quad (2.68)$$

with the elements of the matrices $[A]$ and $[B]$ given by

$$A_{ij} = \sum_{k=1}^N (\bar{Q}_{ij})_K (t_k - t_{k-1}) \quad (i, j = 1, 2, 3) \quad (2.69)$$

$$B_{ij} = \frac{1}{2} \sum_{k=1}^N (\bar{Q}_{ij})_K (t_k^2 - t_{k-1}^2) \quad (i, j = 1, 2, 3) \quad (2.70)$$

The moment resultants are obtained for a K^{th} layer as follows:

$$\begin{Bmatrix} M_x \\ M_y \\ M_{xy} \end{Bmatrix} = \int_{-t/2}^{t/2} \begin{Bmatrix} \sigma_x \\ \sigma_y \\ \sigma_{xy} \end{Bmatrix} z dz \quad (2.71)$$

or,

$$[M] = [B][\epsilon_0] + [D][\kappa] \quad (2.72)$$

$$\text{where } D_{ij} = \frac{1}{3} \sum_{k=1}^N (\bar{Q}_{ij})_K (t_K^3 - t_{K-1}^3) \quad (2.73)$$

D. $[B]$, THE STRAIN-DISPLACEMENT MATRIX

1. Introduction

In this section, we describe how the matrix $[B]$ may be calculated.

The matrix $[B]$, which relates the strains and displacements at nodal points of an element may be obtained in the form,

$$\{\epsilon\} = [B]\{u\} \quad (2.74)$$

It may be observed that this matrix depends on the choice of the nodal degrees of freedom, the shape function and the form of strain-displacement relations.

In the discussion that follows, we describe the nine noded bi-quadratic Lagrangian isoparametric element. There are five degrees of freedom associated with each node.

2. Shape Functions and Their Derivatives

A finite element is called an isoparametric element if the same interpolation functions define both the geometry and displacements.

Figure 2.4 shows the element in the mapped space. For the in-plane deformation, the geometry may be interpolated

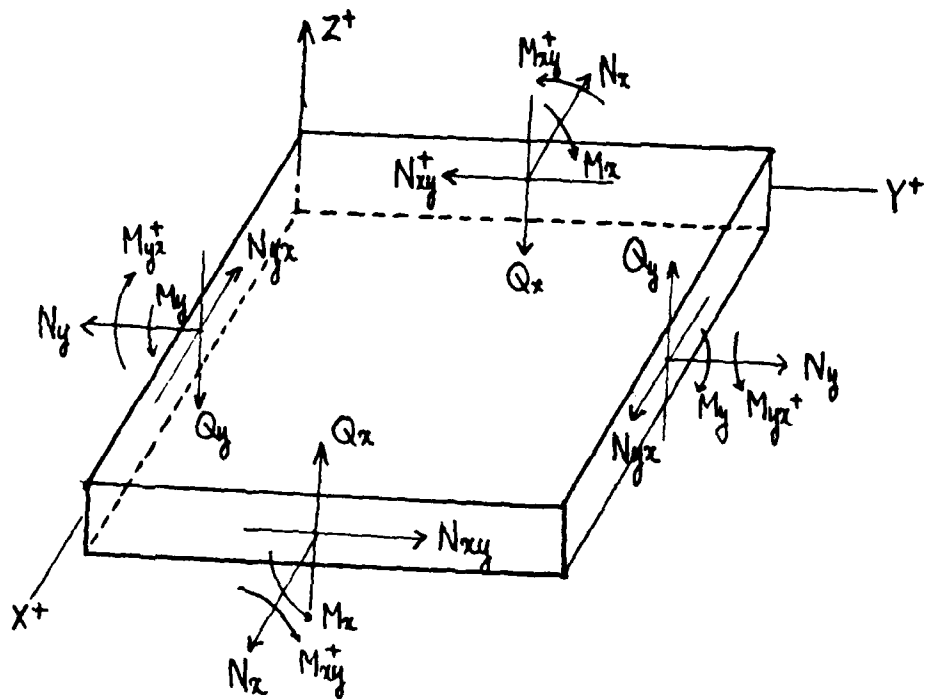


Figure 2.3: Positive Directions for Stress Resultants and Stress Couples for a Lamina

$$\begin{Bmatrix} x \\ y \end{Bmatrix} = [N] \{x_1 y_1 x_2 y_2 \cdots x_9 y_9\} \quad (2.75)$$

and the displacements given by

$$\begin{Bmatrix} u \\ v \end{Bmatrix} = [N] \{u_1 v_1 u_2 v_2 \cdots u_9 v_9\} \quad (2.76)$$

where the matrix of shape functions is given by

$$[N] = \begin{bmatrix} N_1 & 0 & N_2 & 0 & \cdots & N_9 & 0 \\ 0 & N_1 & 0 & N_2 & \cdots & 0 & N_9 \end{bmatrix} \quad (2.77)$$

We may also write the displacements in a summation notation as

$$u = \sum_{i=1}^9 N_i u_i \quad (2.78)$$

$$v = \sum_{i=1}^9 N_i v_i \quad (2.79)$$

In the case of plate bending, three more degrees of freedom are added to the planar displacements.

The transverse displacement w , θ_x and θ_y are the rotations of the normal to the undeformed middle surface in the $x - z$ and $y - z$ plane, respectively.

$$w = \sum_{i=1}^9 N_i w_i \quad (2.80)$$

$$\theta_x = \sum_{i=1}^9 N_i \theta_{xi} \quad (2.81)$$

$$\theta_y = \sum_{i=1}^9 N_i \theta_{yi} \quad (2.82)$$

The shape functions and their derivatives, which are needed for the computations of strains, are given in Table 2.1.

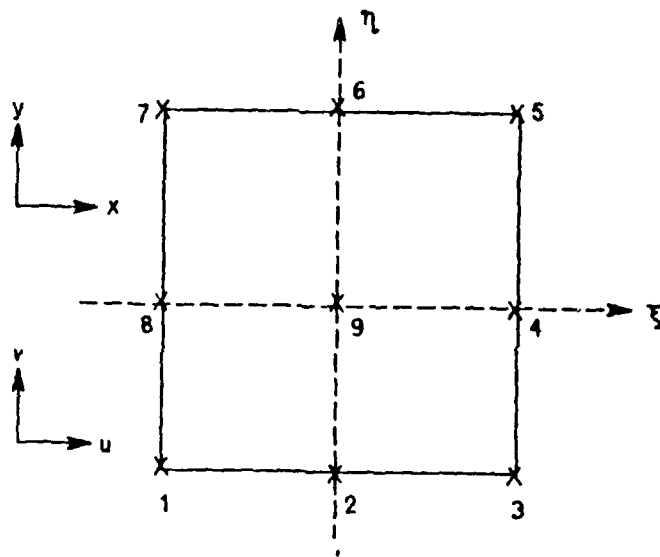


Figure 2.4: Lagrangian Plate Element

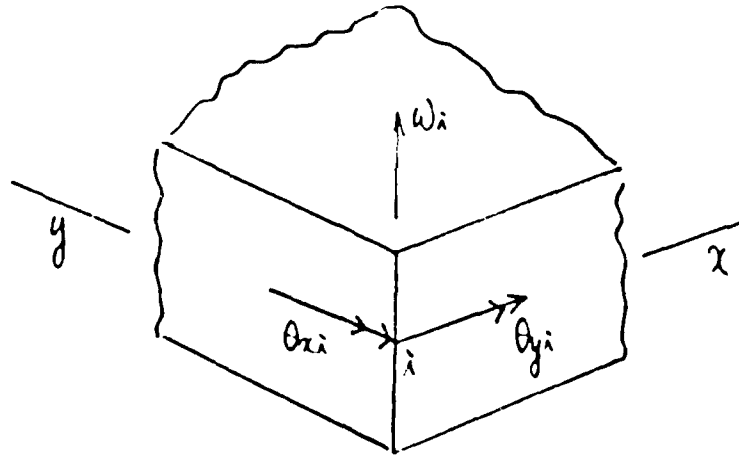


Figure 2.5: Degrees of Freedom at a Typical Node i .

It may be noted that the rotational degrees of freedom are treated as independent quantities, following Mindlin theory [Refs. 37, 38, 39].

3. Jacobian Transformation Matrix

The chain rules for differentiation of $N(\xi, \eta)$ with respect to ξ and η gives,

$$\frac{\partial N_i}{\partial \xi} = \frac{\partial N_i}{\partial x} \frac{\partial x}{\partial \xi} + \frac{\partial N_i}{\partial y} \frac{\partial y}{\partial \xi} \quad (2.83)$$

$$\frac{\partial N_i}{\partial \eta} = \frac{\partial N_i}{\partial x} \frac{\partial x}{\partial \eta} + \frac{\partial N_i}{\partial y} \frac{\partial y}{\partial \eta} \quad (2.84)$$

or, in matrix form,

$$\begin{bmatrix} \frac{\partial N_i}{\partial \xi} \\ \frac{\partial N_i}{\partial \eta} \end{bmatrix} = \begin{bmatrix} \frac{\partial x}{\partial \xi} & \frac{\partial y}{\partial \xi} \\ \frac{\partial x}{\partial \eta} & \frac{\partial y}{\partial \eta} \end{bmatrix} \begin{bmatrix} \frac{\partial N_i}{\partial x} \\ \frac{\partial N_i}{\partial y} \end{bmatrix} \quad (2.85)$$

The Cartesian derivatives are given by

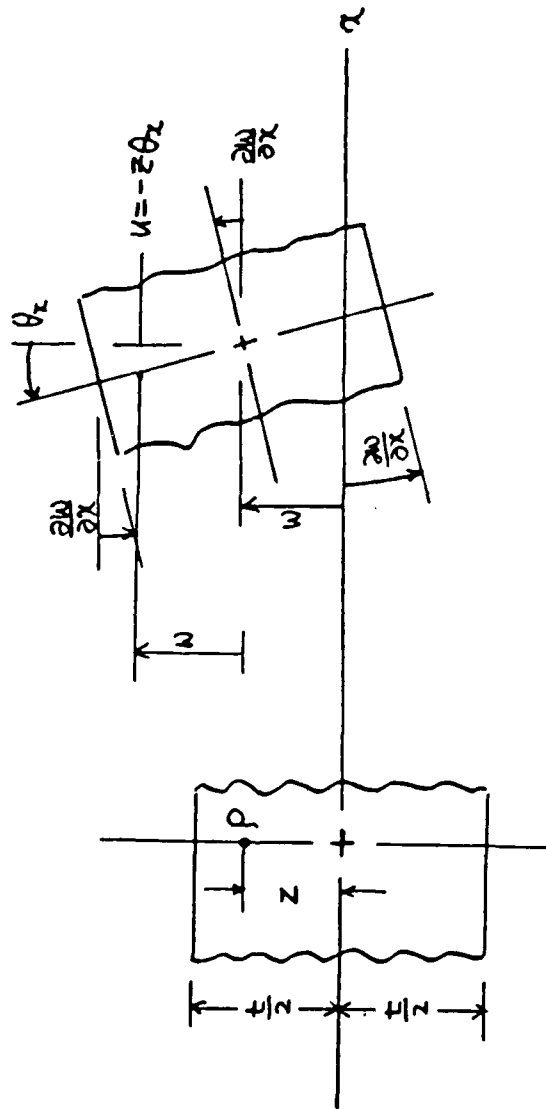


Figure 2.6: Displacements in the $x-z$ Plane

	$\{N\}$	$\{CN/\xi\}$	$\{CN,\xi\eta\}$
1	$\frac{(1-\xi)(1-\eta)\xi\eta}{4}$	$\frac{(1-2\xi)(1-\eta)\eta}{4}$	$\frac{(1-\xi)(1-2\eta)\xi}{4}$
2	$-\frac{(1-\xi^2)(1-\eta)\eta}{2}$	$(1-\eta)\xi\eta$	$-\frac{(1-\xi^2)(1-2\eta)}{2}$
3	$-\frac{(1+\xi)(1-\eta)\xi\eta}{4}$	$-\frac{(1+2\xi)(1-\eta)\eta}{4}$	$-\frac{(1+\xi)(1-2\eta)\xi}{4}$
4	$\frac{(1+\xi)(1-\eta^2)\xi}{2}$	$\frac{(1+2\xi)(1-\eta^2)}{2}$	$-(1+\xi)\xi\eta$
5	$\frac{(1+\xi)(1+\eta)\xi\eta}{4}$	$\frac{(1+2\xi)(1+\eta)\eta}{4}$	$\frac{(1+\xi)(1+2\eta)\xi}{4}$
6	$\frac{(1-\xi^2)(1+\eta)\eta}{2}$	$-(1+\eta)\xi\eta$	$\frac{(1-\xi^2)(1+2\eta)}{2}$
7	$-\frac{(1-\xi)(1+\eta)\xi\eta}{4}$	$-\frac{(1-2\xi)(1+\eta)\eta}{4}$	$-\frac{(1-\xi)(1+2\eta)\xi}{4}$
8	$-\frac{(1-\xi)(1-\eta^2)\xi}{2}$	$-\frac{(1-2\xi)(1-\eta^2)}{2}$	$(1-\xi)\xi\eta$
9	$(1-\xi^2)(1-\eta^2)$	$-2(1-\eta^2)\xi$	$-2(1-\xi^2)\eta$

TABLE 2.1: Shape Function and Their Derivatives

$$\begin{bmatrix} \frac{\partial N_i}{\partial x} \\ \frac{\partial N_i}{\partial y} \end{bmatrix} = \begin{bmatrix} \frac{\partial x}{\partial \xi} & \frac{\partial y}{\partial \xi} \\ \frac{\partial x}{\partial \eta} & \frac{\partial y}{\partial \eta} \end{bmatrix}^{-1} \begin{bmatrix} \frac{\partial N_i}{\partial \xi} \\ \frac{\partial N_i}{\partial \eta} \end{bmatrix} \quad (2.86)$$

The Jacobian matrix $[J]$, which contains the derivatives of the global coordinates with respect to the local coordinates is given by,

$$[J] = \begin{bmatrix} \frac{\partial x}{\partial \xi} & \frac{\partial y}{\partial \xi} \\ \frac{\partial x}{\partial \eta} & \frac{\partial y}{\partial \eta} \end{bmatrix} \quad (2.87)$$

By using isoparametric element concepts [Ref. 1], we may write the Jacobian elements as,

$$J_{11} = \sum_{i=1}^9 \frac{\partial N_i}{\partial \xi} x_i \quad (2.88)$$

$$J_{12} = \sum_{i=1}^9 \frac{\partial N_i}{\partial \xi} y_i \quad (2.89)$$

$$J_{21} = \sum_{i=1}^9 \frac{\partial N_i}{\partial \eta} x_i \quad (2.90)$$

$$J_{22} = \sum_{i=1}^9 \frac{\partial N_i}{\partial \eta} y_i \quad (2.91)$$

The inverse of the Jacobian matrix can be expressed as

$$[J]^{-1} = \frac{1}{|J|} \begin{bmatrix} J_{22} & -J_{12} \\ -J_{21} & J_{11} \end{bmatrix} \quad (2.92)$$

with the determinant of the Jacobian given by

$$|J| = J_{11}J_{22} - J_{21}J_{12} \quad (2.93)$$

The Cartesian derivatives are, then, given by

$$\frac{\partial N_i}{\partial x} = \frac{1}{|J|} \left(J_{22} \frac{\partial N_i}{\partial \xi} - J_{12} \frac{\partial N_i}{\partial \eta} \right) \quad (2.94)$$

$$\frac{\partial N_i}{\partial y} = \frac{1}{|J|} \left(-J_{21} \frac{\partial N_i}{\partial \xi} + J_{11} \frac{\partial N_i}{\partial \eta} \right) \quad (2.95)$$

4. Formation of [B] Matrix

The equation (2.74) may be written as

$$\begin{bmatrix} \epsilon_x \\ \epsilon_y \\ \gamma_{xy} \end{bmatrix} = \begin{bmatrix} \frac{\partial}{\partial x} & 0 \\ 0 & \frac{\partial}{\partial y} \\ \frac{\partial}{\partial y} & \frac{\partial}{\partial x} \end{bmatrix} \begin{Bmatrix} u \\ v \end{Bmatrix} \quad (2.96)$$

Replacing the displacements in terms of nodal displacements, we get

$$\begin{bmatrix} \epsilon_x \\ \epsilon_y \\ \gamma_{xy} \end{bmatrix} = \begin{bmatrix} \frac{\partial \sum N_i}{\partial x} & 0 \\ 0 & \frac{\partial \sum N_i}{\partial y} \\ \frac{\partial \sum N_i}{\partial y} & \frac{\partial \sum N_i}{\partial x} \end{bmatrix} \begin{Bmatrix} u_i \\ v_i \end{Bmatrix} \quad (2.97)$$

or, in matrix form

$$\{\epsilon\} = [B_i] \{u\} \quad (2.98)$$

where $[B_i]$ is given by

$$[B_i] = \begin{bmatrix} \frac{\partial N_i}{\partial x} & 0 \\ 0 & \frac{\partial N_i}{\partial y} \\ \frac{\partial N_i}{\partial y} & \frac{\partial N_i}{\partial x} \end{bmatrix} \quad (2.99)$$

For plate bending, we have,

$$\begin{bmatrix} \epsilon_z \\ \epsilon_y \\ \gamma_{xy} \end{bmatrix} = \begin{bmatrix} 0 & \frac{\partial}{\partial x} & 0 \\ 0 & 0 & \frac{\partial}{\partial y} \\ 0 & \frac{\partial}{\partial y} & \frac{\partial}{\partial x} \end{bmatrix} \begin{Bmatrix} w \\ u \\ v \end{Bmatrix} \quad (2.100)$$

or, in terms of nodal displacements,

$$\begin{bmatrix} \epsilon_x \\ \epsilon_y \\ \gamma_{xy} \end{bmatrix} = \begin{bmatrix} 0 & -\frac{\partial \sum N_i}{\partial x} & 0 \\ 0 & 0 & -\frac{\partial \sum N_i}{\partial y} \\ 0 & -\frac{\partial \sum N_i}{\partial y} & -\frac{\partial \sum N_i}{\partial x} \end{bmatrix} \begin{Bmatrix} \omega_i \\ \theta_{xi} \\ \theta_{yi} \end{Bmatrix} \quad (2.101)$$

The transverse shears are expressed by

$$\begin{bmatrix} \gamma_{yz} \\ \gamma_{zx} \end{bmatrix} = \begin{bmatrix} \frac{\partial}{\partial y} & 0 & 1 \\ \frac{\partial}{\partial x} & 1 & 0 \end{bmatrix} \begin{Bmatrix} \sum N_i \omega_i \\ -\sum N_i \theta_{xi} \\ -\sum N_i \theta_{yi} \end{Bmatrix} \quad (2.102)$$

or,

$$\begin{bmatrix} \gamma_{yz} \\ \gamma_{zx} \end{bmatrix} = \begin{bmatrix} \frac{\partial \sum N_i}{\partial y} & 0 & -\sum N_i \\ \frac{\partial \sum N_i}{\partial x} & -\sum N_i & 0 \end{bmatrix} \begin{Bmatrix} \omega_i \\ \theta_{xi} \\ \theta_{yi} \end{Bmatrix} \quad (2.103)$$

We may write $[B_i]$ for plate elements as

$$[B_i] = \begin{bmatrix} 0 & -\frac{\partial N_i}{\partial x} & 0 \\ 0 & 0 & -\frac{\partial N_i}{\partial y} \\ 0 & -\frac{\partial N_i}{\partial y} & -\frac{\partial N_i}{\partial x} \\ \frac{\partial N_i}{\partial y} & 0 & -N_i \\ \frac{\partial N_i}{\partial x} & -N_i & 0 \end{bmatrix} \quad (2.104)$$

E. GAUSSIAN QUADRATURE

1. Introduction

In this section, we discuss aspects of numerical integration. Here we describe the Gaussian method to calculate the integrals, which is widely used in finite element work [Refs. 38, 39].

2. Summary of Gauss Quadrature

To approximate an integral I ,

$$I = \int_{-1}^1 \phi d\xi \quad (2.105)$$

where $\phi(\xi)$ is a function defined in that region. As shown in the Figure 2.7, we sample ϕ at the midpoint of the interval and multiply by the length of the interval.

Generalization of Equation (2.105) leads to the formula

$$I = \sum_{i=1}^n W_i \phi(\xi_i) \quad (2.106)$$

or,

$$I = W_1 \phi(\xi_1) + W_2 \phi(\xi_2) + \cdots + W_n \phi(\xi_n) \quad (2.107)$$

where ξ_i is the location of the integration point i with respect to the origin, W_i is the weighting factor for point i and n is the number of points at which $\phi(\xi)$ is to be evaluated.

The sampling points and weights for Gaussian Quadrature, which is adapted in the present study, are listed in Table 2.2.

In two dimensions, we may approximate I by

$$I = \sum_i \sum_j W_i W_j \phi(\xi_x, \eta_j) \quad (2.108)$$

In Equation (2.6) and (2.7) each coefficient in the integrand matrix must be integrated as described above.

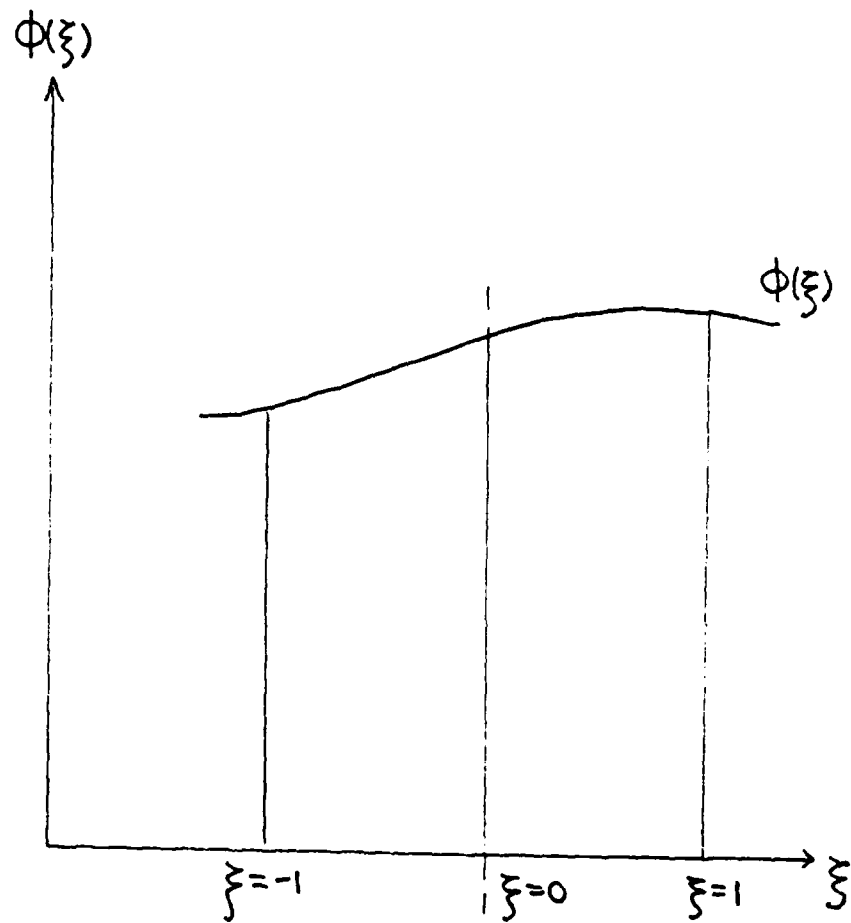


Figure 2.7: Gaussian Quadrature (ξ Coordinate) using Three Sampling Points

n	$\pm \xi_i$	R_i
1	0 0	2 0
2	0 5773502692	1 0
3	0 7745966692 0 0	0 5555555556 0 8888888889
4	0 8611363116 0 3399810436	0 3478548451 0 6521451549
5	0 9061798459 0 5384693101 0 0	0 2369268851 0 4786286705 0 5088888889
6	0 9324695142 0 6612093865 0 2386191861	0 1713244924 0 3607615730 0 4679139346
7	0 9491079123 0 7415311856 0 4058451514 0 0	0 1294849662 0 2797053915 0 3818300505 0 4179591537
8	0 9602898565 0 7960664774 0 5255324099 0 1834346425	0 1012285363 0 2223810345 0 3137066459 0 3626837834

TABLE 2.2: Coefficients for Gaussian Quadrature

III. PROGRAM IMPLEMENTATION

A. INTRODUCTION

After having formed the element stiffness matrices, the global matrices are formed in a standard manner [Refs. 1, 38], resulting in, for static analysis,

$$\{F\} = [K] \{u\}$$

where $\{F\}$: External loads vector
 $\{K\}$: Stiffness matrix
 $\{u\}$: Nodal displacements vector

If we know $\{F\}$ and $[K]$, $\{u\}$ may be computed for a static problem. Typical steps for static analysis may be described as follows:

Step 1: Input the material properties, plate coordinates, loads, the number of integration points, boundary conditions.

Step 2: For the composite, input number of layers, elements and fiber orientations.

Step 3: Determine element matrices in global coordinate system.

Step 4: Assemble the element matrices.

Step 5: Solve for displacements and stresses.

The Figure 3.1 shows the flow chart of the program.

B. SOLUTION PROCEDURE

In order to obtain numerical solution, the element matrices were programmed and incorporated into an existing finite element program. The implementation in double precision was done on a 32-bit Apollo D-3000 series computer.

Following steps describe the element subroutine.

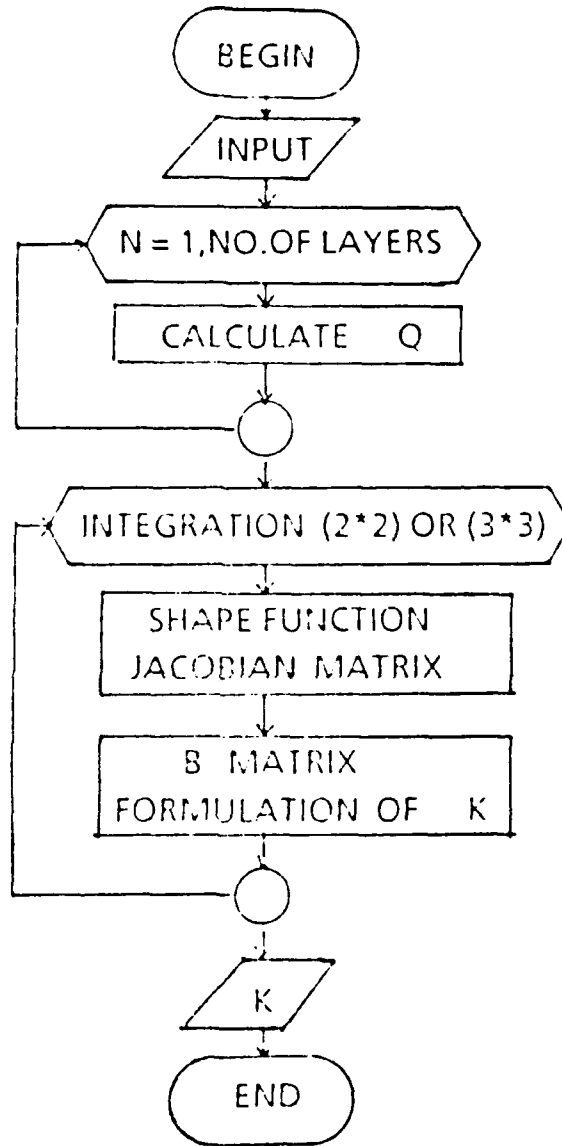


Figure 3.1: Flow Chart (Main Program)

Step 1: Material properties from main program are read.

Step 2: Calculate $[Q]$ according to number of layers.

Step 3: Select integration point 2×2 or 3×2 or 3×3 .

Step 4: Establish shape function.

Step 5: Determine the Jacobian matrix and $[B]$.

Step 6: Formulation of $[K]$.

Step 7: For each integration point, do steps 4, 5, and 6, and accumulate $[K]$.

Step 8: Calculate $[K]$ for each element.

Step 9: Return to main program.

The flow chart for element level computation is given in Figure 3.2.

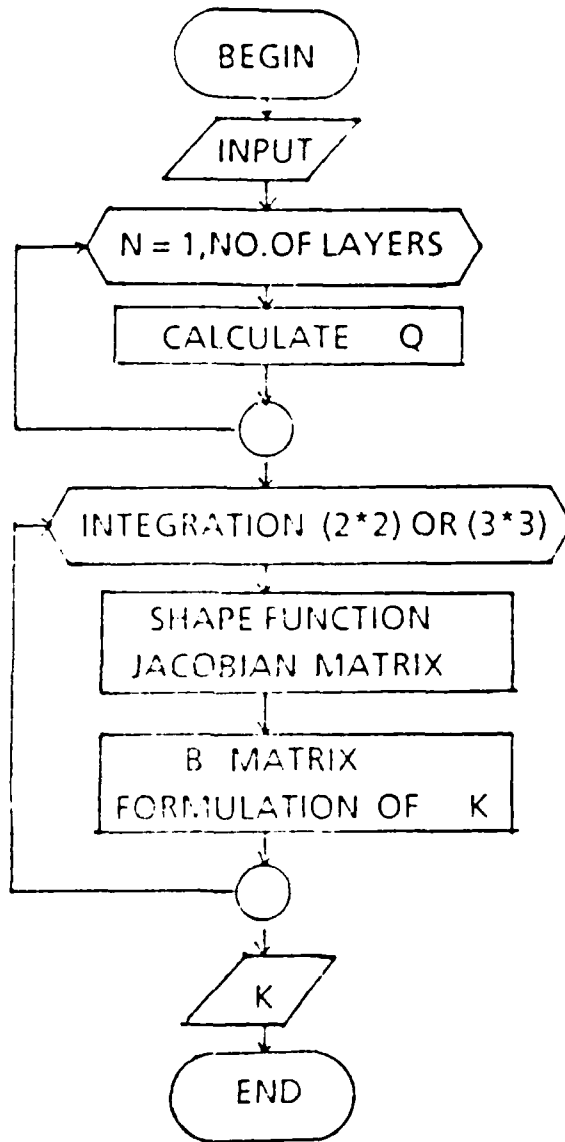


Figure 3.2: Flow Chart (KQML9)

IV. NUMERICAL EXAMPLES

A. INTRODUCTION

This section discusses the validation of the element formulation and implementation by means of selected numerical examples. The isotropic elastic plates are solved under different boundary conditions and loadings.

This is followed by application to selected laminated composite plates to check the formulation for such applications. The effects of thickness and integration schemes also are investigated.

B. SIMPLY SUPPORTED SQUARE ISOTROPIC PLATE

1. Simply supported plate under concentrated load.

Consider a rectangular isotropic plate under a central point load. The geometry and the boundary conditions are shown in the Figure 4.1. The structure is modeled using the double symmetry.

The properties of material I are given by

$$E = 10.92 \times 10^6 \text{ (psi)}$$

$$\nu = 0.3$$

$$L = 10 \text{ in}$$

$$P = 400 \text{ (lbs)}$$

The geometric boundary conditions of the simply supported plate are $w = 0$ on all edges.

As shown in the Figure 4.2, results depicting maximum displacement obtained using 2×2 integration points, 3×3 integration points and 'heterosis' [Ref. 4] elements are compared. As the thickness decreases, the element is more effective for integration schemes and for thick plates, the error is approximately 20%. It is possible that by increasing the number of elements, it may improve the solution.

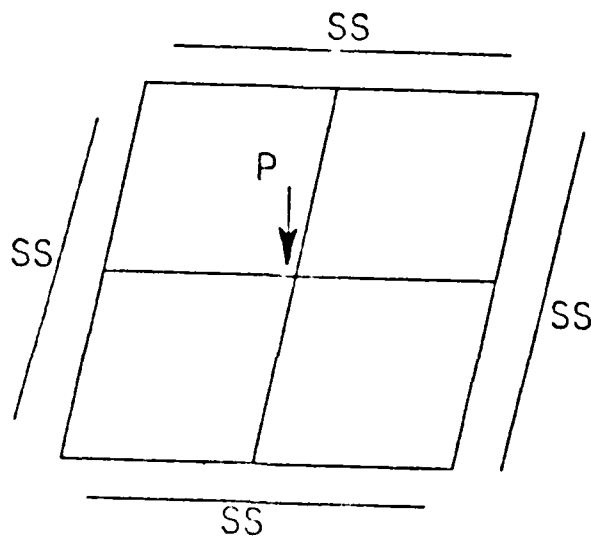


Figure 4.1: A Rectangular Isotropic Plate under Concentrated Point Load

W/W_{anal} vs. No. of elements are shown in Figure 4.3. As the number of elements are increased, the solution converges to the analytically predicted values. It may be noted that reduced order of integration is more flexible, and approaches the analytical solution as an upper bound.

2. Simply Supported Plate under Distributed Load

Next we consider a rectangular plate under a distributed load. The geometry and the boundary conditions are the same as in the previous example. The model of the structure, using the symmetry, is shown in Figure 4.4.

The material properties for this example are given earlier as material I.

The normalized maximum deflection is shown plotted against the number of elements in Figure 4.5. It may be observed that different integration schemes converge towards a lower bound. Figure 4.6 depicts the effectiveness of this element in predicting behavior of thick and thin plates.

This element gives better predictions for thick plates than heterosis element, however, for thin plates, heterosis element appears to be better.

C. CLAMPED-CLAMPED SQUARE ISOTROPIC PLATE

Consider a rectangular plate clamped on all sides, under a distributed load. The geometry and boundary conditions are shown in Figure 4.7. The boundary conditions for this problem are implemented by prescribing all degrees of freedom to zero, on all four edges. The structure, again, is modeled using the symmetry.

The material properties for this plate are same as for material I.

The results showing the normalized maximum displacements are shown in Figure 4.8. The heterosis element results in about ten percent error while the Lagrangian element gives about twenty to twenty-three percent for thick plates.

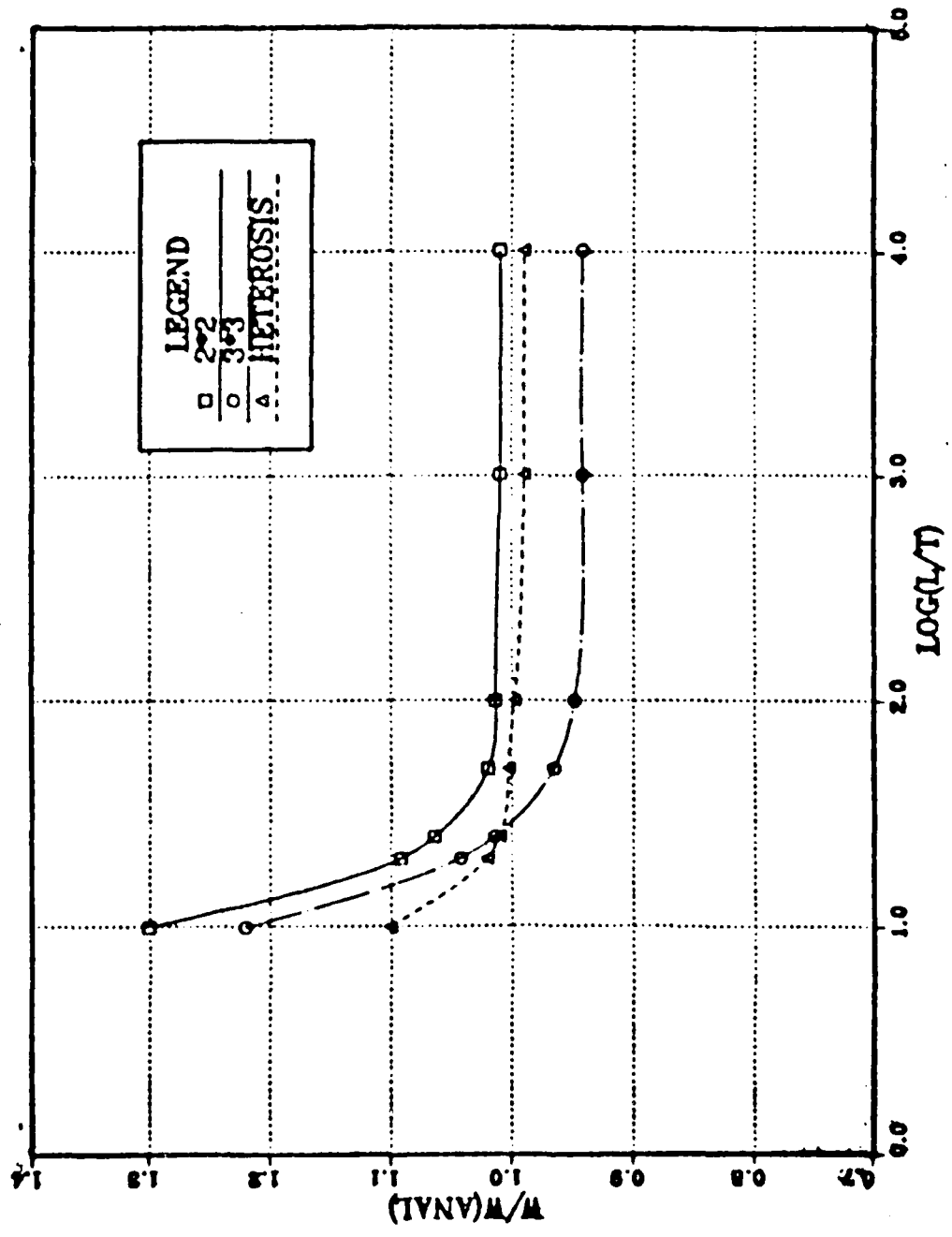


Figure 4.2: W/W_{anal} vs. $\text{Log}(L/T)$ on Simply Supported Square Plate under Central Point Load.

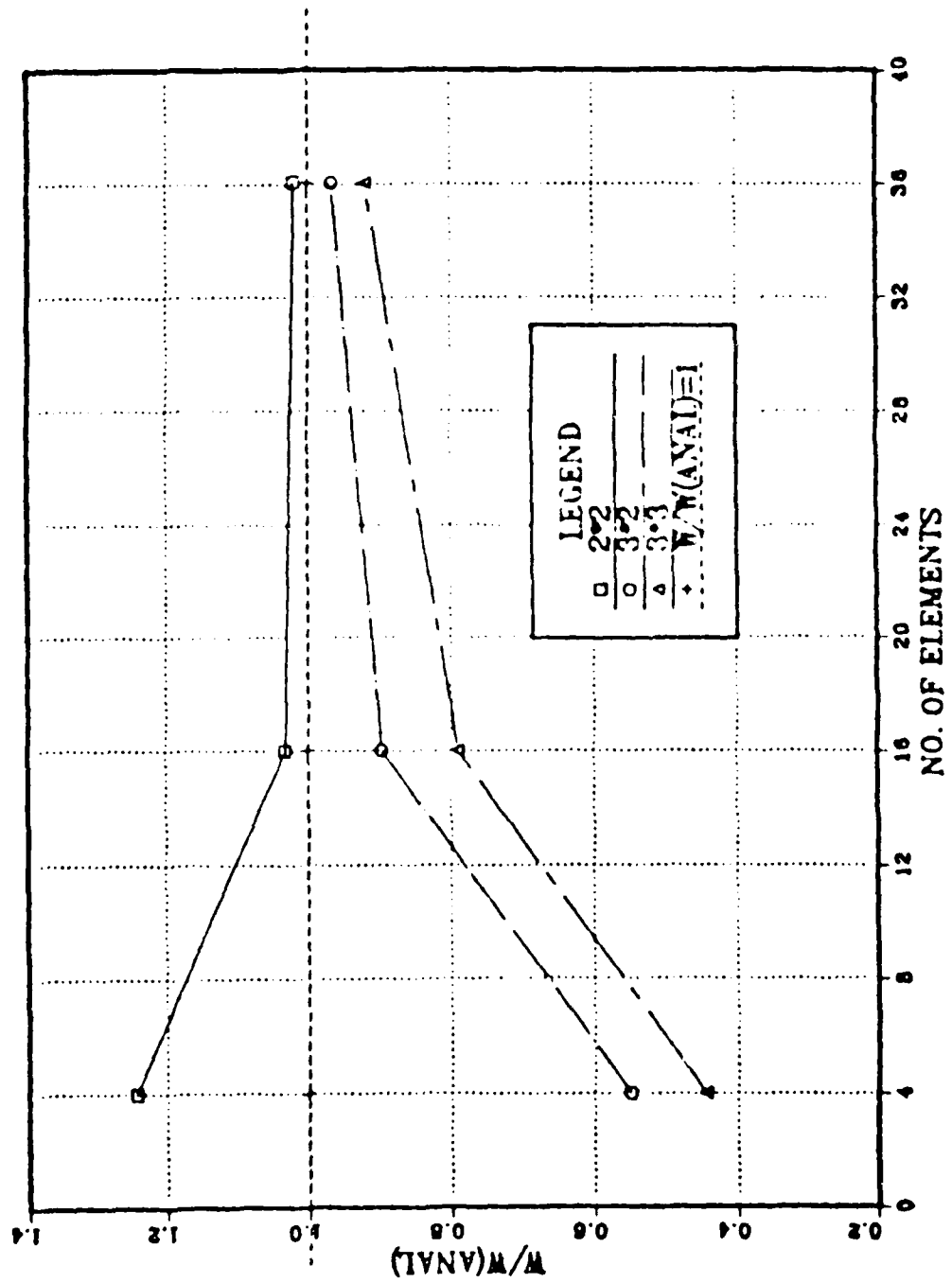


Figure 4.3: W/W_{anal} vs. No. of Elements on Simply Supported Square Plate under Central Point Load.

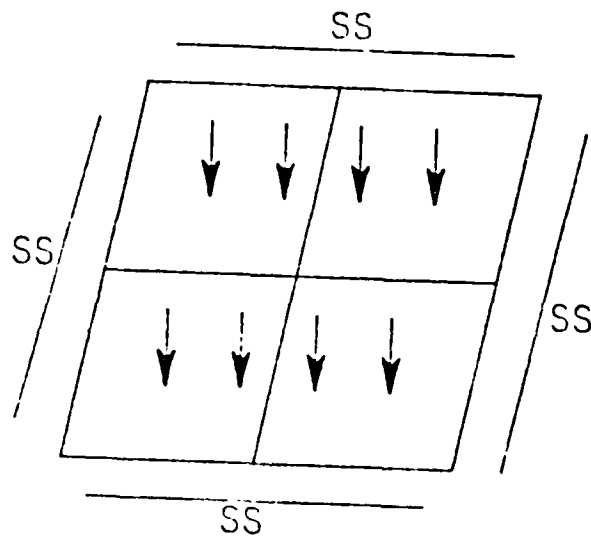


Figure 4.4: A Rectangular Isotropic Plate under Distributed Load

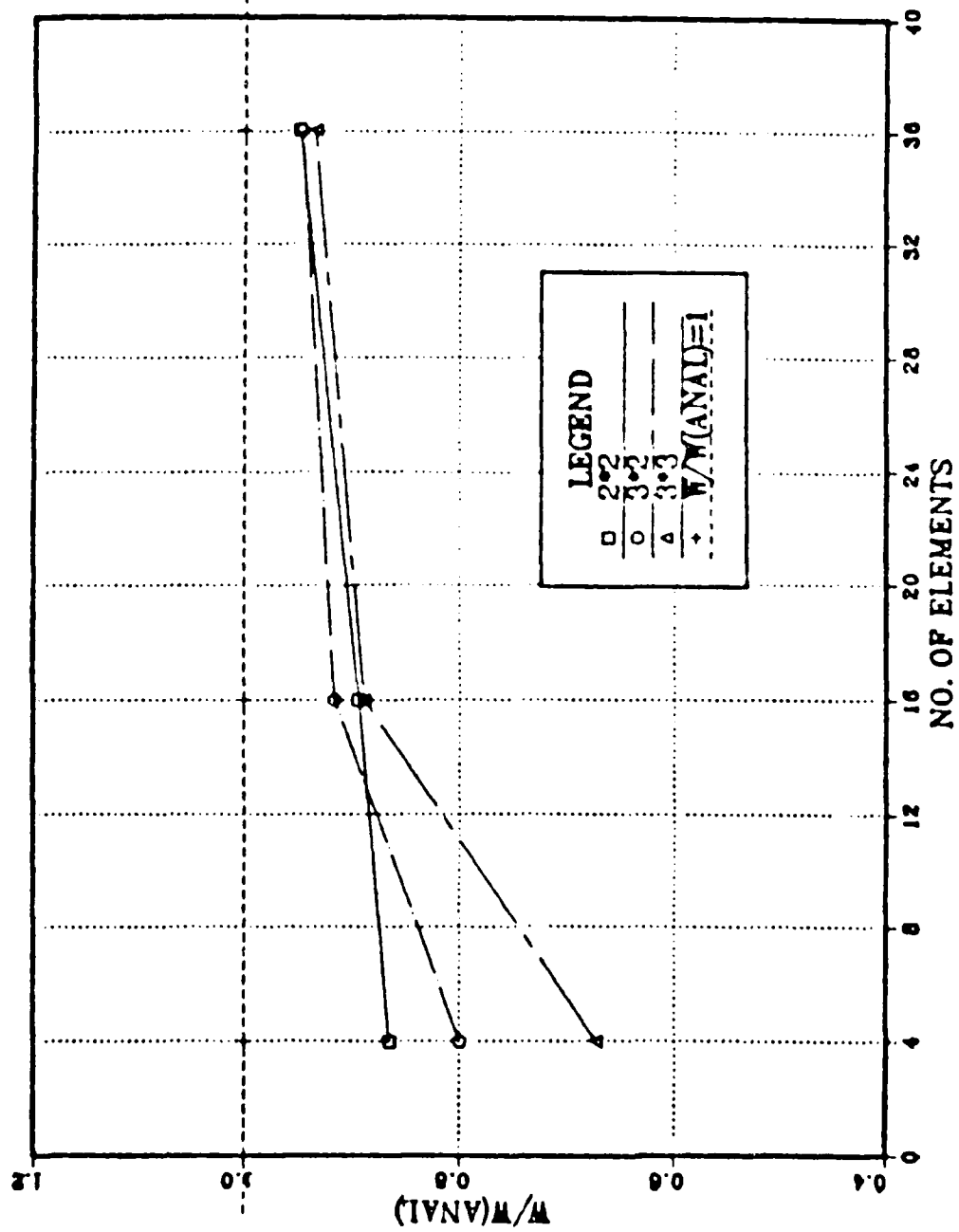


Figure 4.5: $W/W_{(anal)}$ vs. No. of Elements on Simply Supported Plate Under Distributed Load

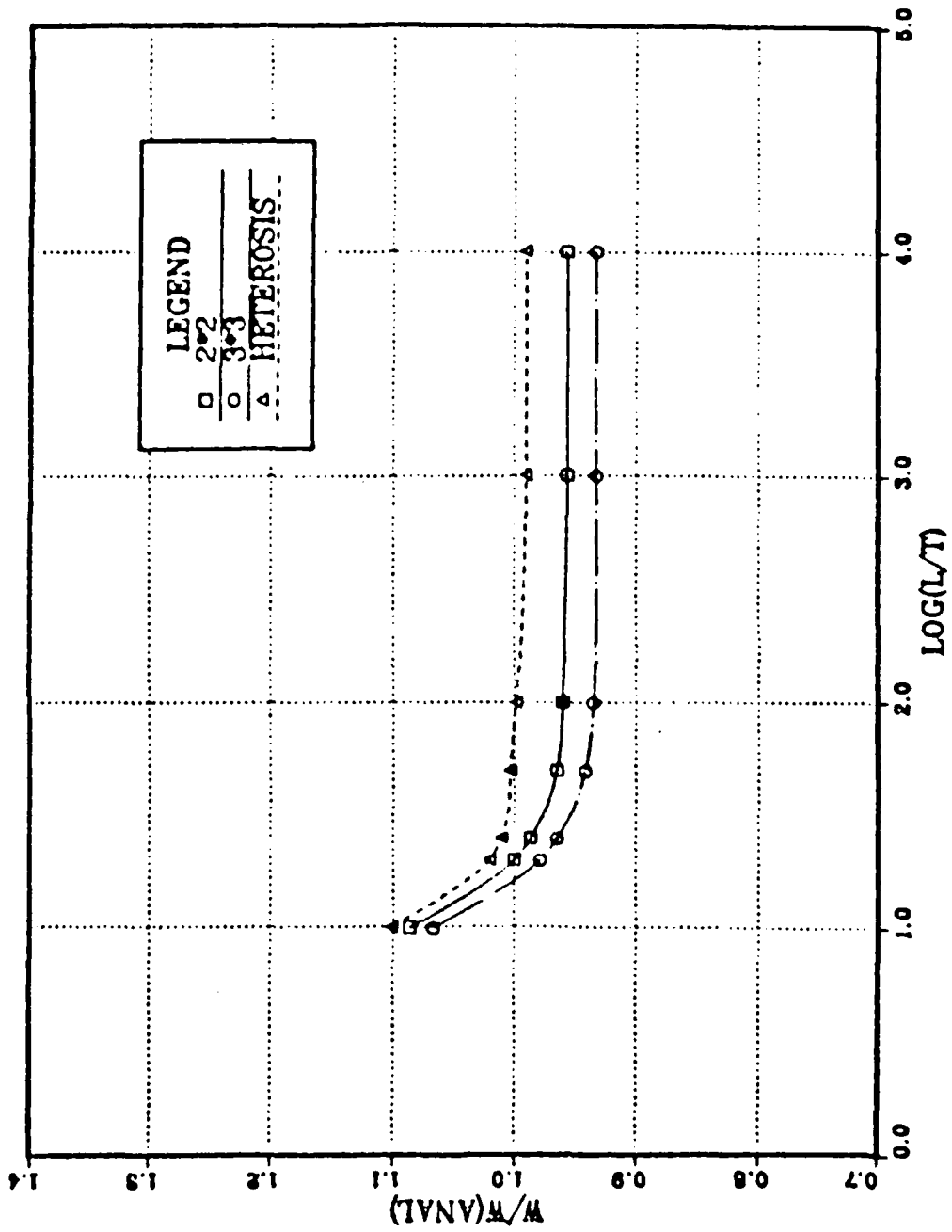


Figure 4.6: $W/W_{(anal)}$ vs. $\text{Log}(L/T)$ on Simply Supported Plate Under Distributed Load

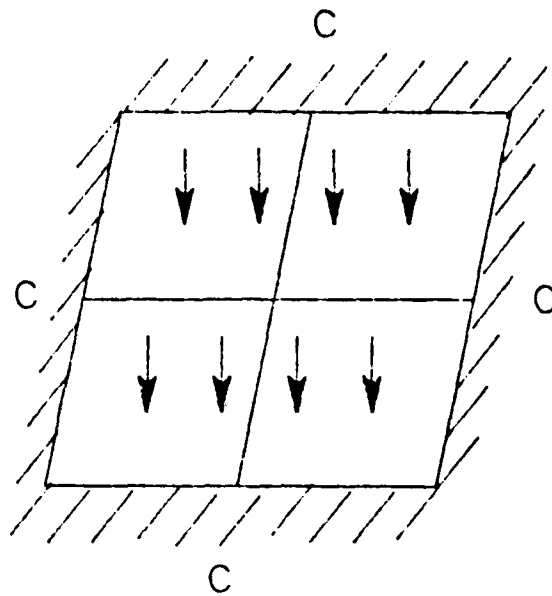


Figure 4.7: A Clamped-Clamped Rectangular Plate Under Distributed Load

However, for thin plates, the predictions are about the same using either elements. Figure 4.9 shows the convergence characteristics of the element.

D. CANTILEVERED ISOTROPIC PLATE

Next example considered is a cantilevered plate. The geometry and boundary conditions are shown in the Figure 4.10. The material properties, (material II), are given by

$$E = 1 \times 10^4 (k/in^2) \quad (4.1)$$

$$\nu = 0.3 \quad (4.2)$$

$$L = 10(in) \quad (4.3)$$

$$t = 0.2(in) \quad (4.4)$$

The result of this example is shown in the Figure 4.11. As the number of elements is increased, the results converge, for all integration schemes.

E. SIMPLY SUPPORTED LAMINATED PLATE

1. Graphite-epoxy

Consider a rectangular composite plate under a sinusoidal load. Two types of construction are used.

Case I : Graphite-Epoxy $0^\circ/90^\circ/90^\circ/0^\circ$

Case II : Graphite-Epoxy $0^\circ/-60^\circ/60^\circ/0^\circ$

Material properties are given by

$$\frac{G_{12}}{E_2} = 0.6 \quad (4.5)$$

$$\frac{G_{22}}{E_2} = 0.5 \quad (4.6)$$

$$\nu_{12} = 0.25 \quad (4.7)$$

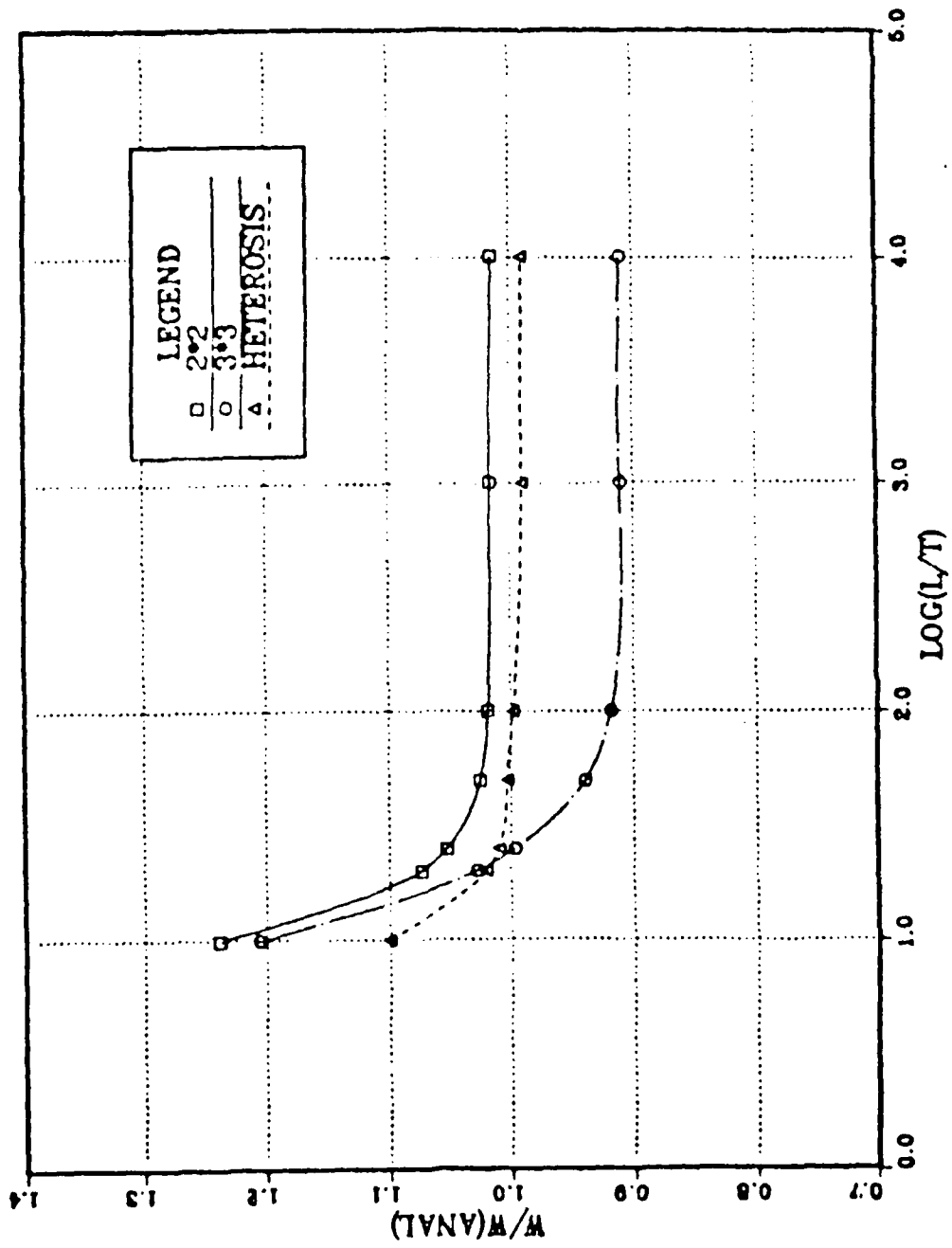


Figure 4.8: $W/W_{(anal)}$ vs. $Log(L/T)$ for Clamped-Clamped Plate under Distributed Load

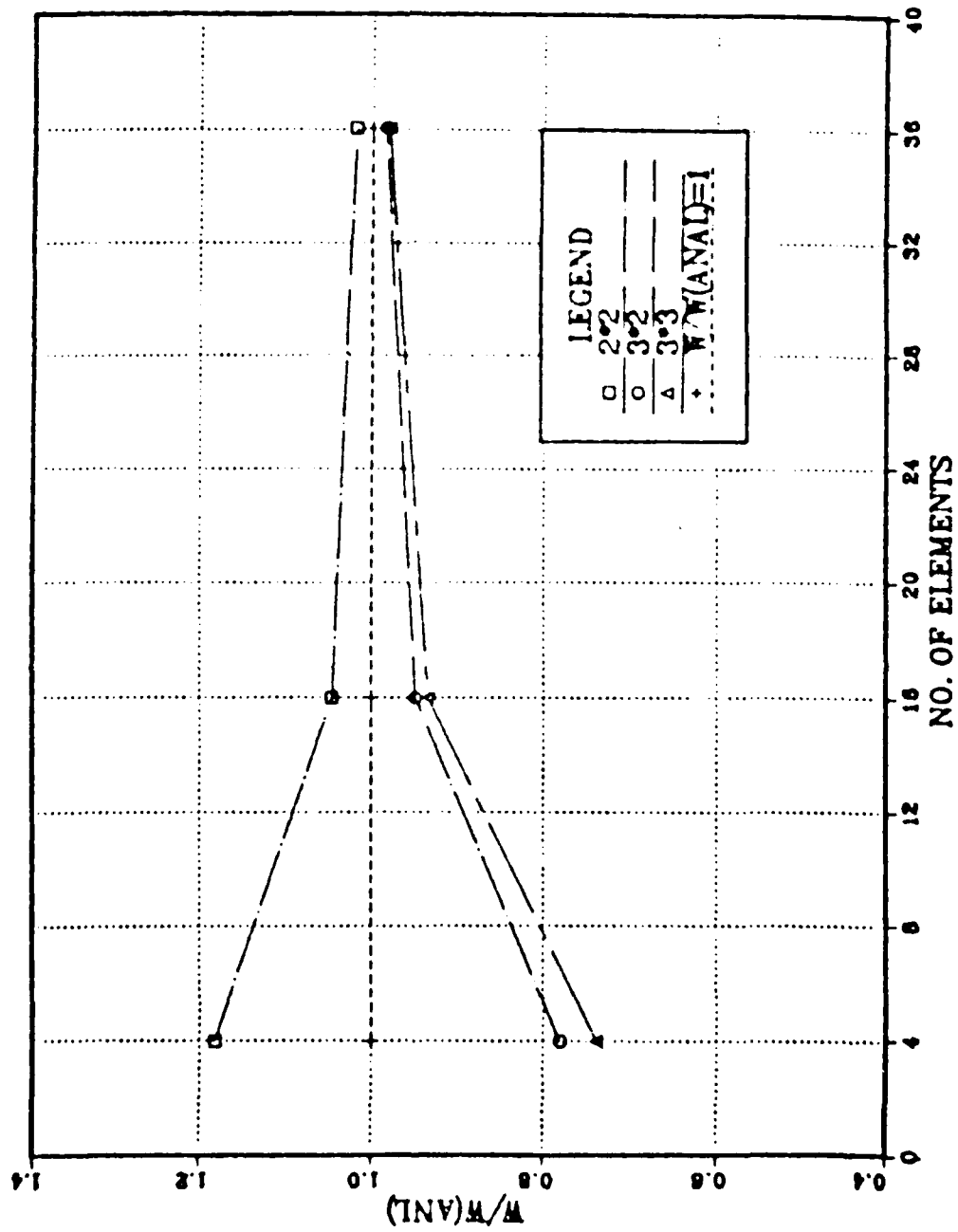


Figure 4.9: Nondimensional Deflection vs. No. of Element for Clamped-Clamped Plate under Distributed Load

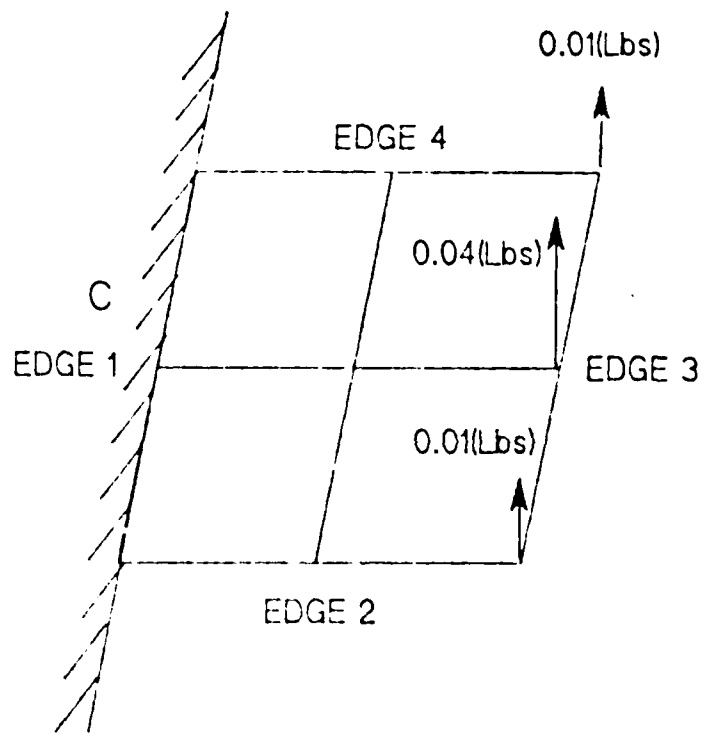


Figure 4.10: Cantilevered Plate

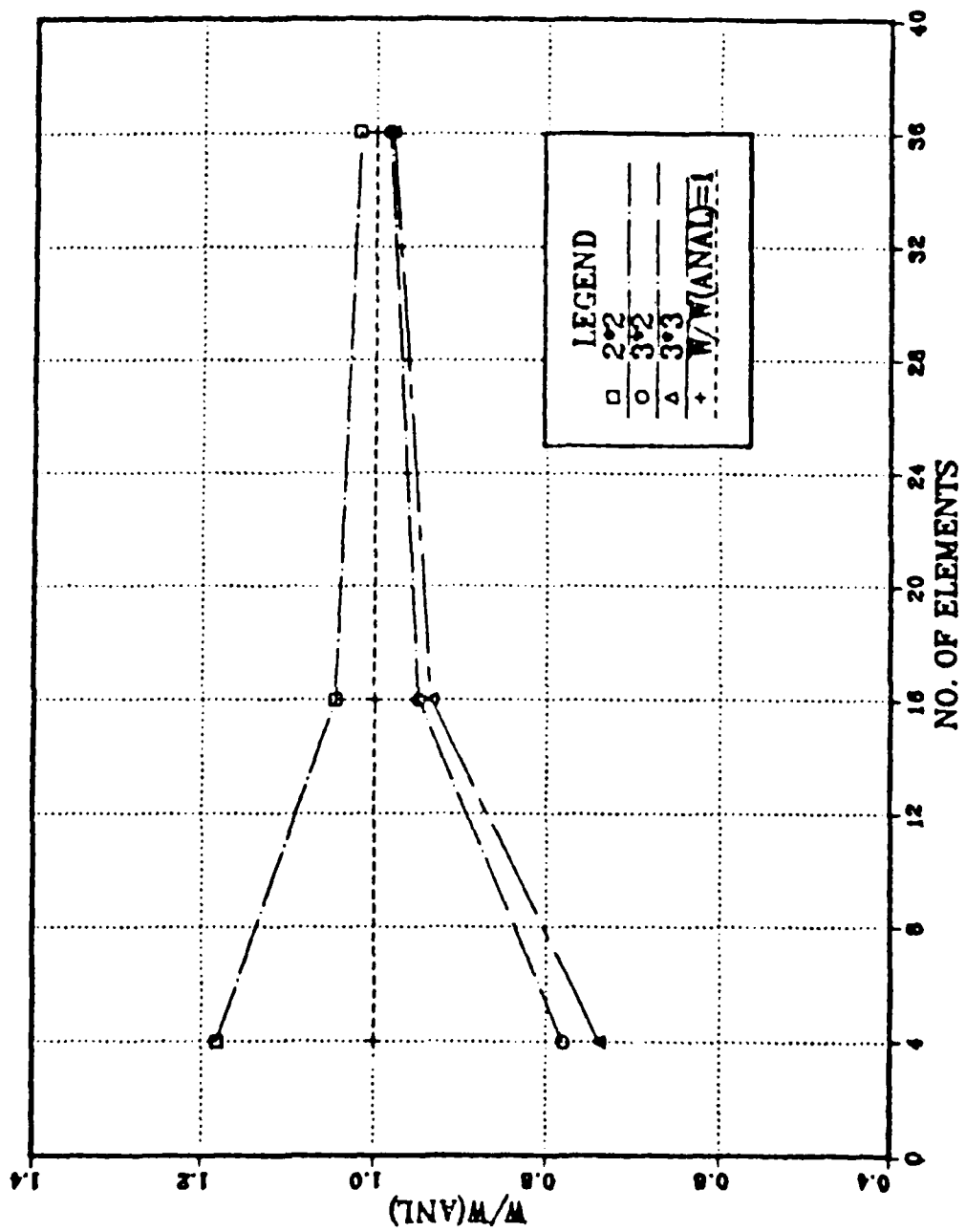


Figure 4.11: $W/W_{(anal)}$ vs. No. of Element for Cantilevered Plate

$$\frac{E_1}{E_2} = 40 \quad (4.8)$$

The plate is subjected to a transverse sinusoidal load of intensity

$$q = q_0 \sin \frac{\pi x}{L} \sin \frac{\pi y}{L} \quad (4.9)$$

This problem is studied to compare finite element results with those of shear deformation theory [Ref. 24] and elasticity solution [Refs. 16, 17, 18]. The results are in Figure 4.12 for Case I. The deflection obtained from the finite element solutions agree very well with the exact elasticity solutions. The solutions agree well for thin plates, while a large discrepancy between the present predictions and Reference 24 is observed.

The maximum deflection is plotted as the number of elements are increased in Figure 4.13. The convergence trend may be noted as the number of elements are increased. In Figure 4.14, the results for the second type of composite ($0^\circ / -60^\circ / 60^\circ / 0^\circ$) is depicted.

2. Glass-Epoxy

This section considers rectangular composite plate under sinusoidal load. The two types of construction are Case III, $0^\circ / 90^\circ / 90^\circ / 0$ and Case IV, $0^\circ / -60^\circ / 60^\circ / 0^\circ$. The plates are square and simply supported.

The material properties are given by

$$\frac{E_{12}}{E_2} = 0.6 \quad (4.10)$$

$$\frac{G_{22}}{E_2} = 0.5 \quad (4.11)$$

$$\nu_{12} = 0.25 \quad (4.12)$$

$$\frac{E_1}{E_2} = 3 \quad (4.13)$$

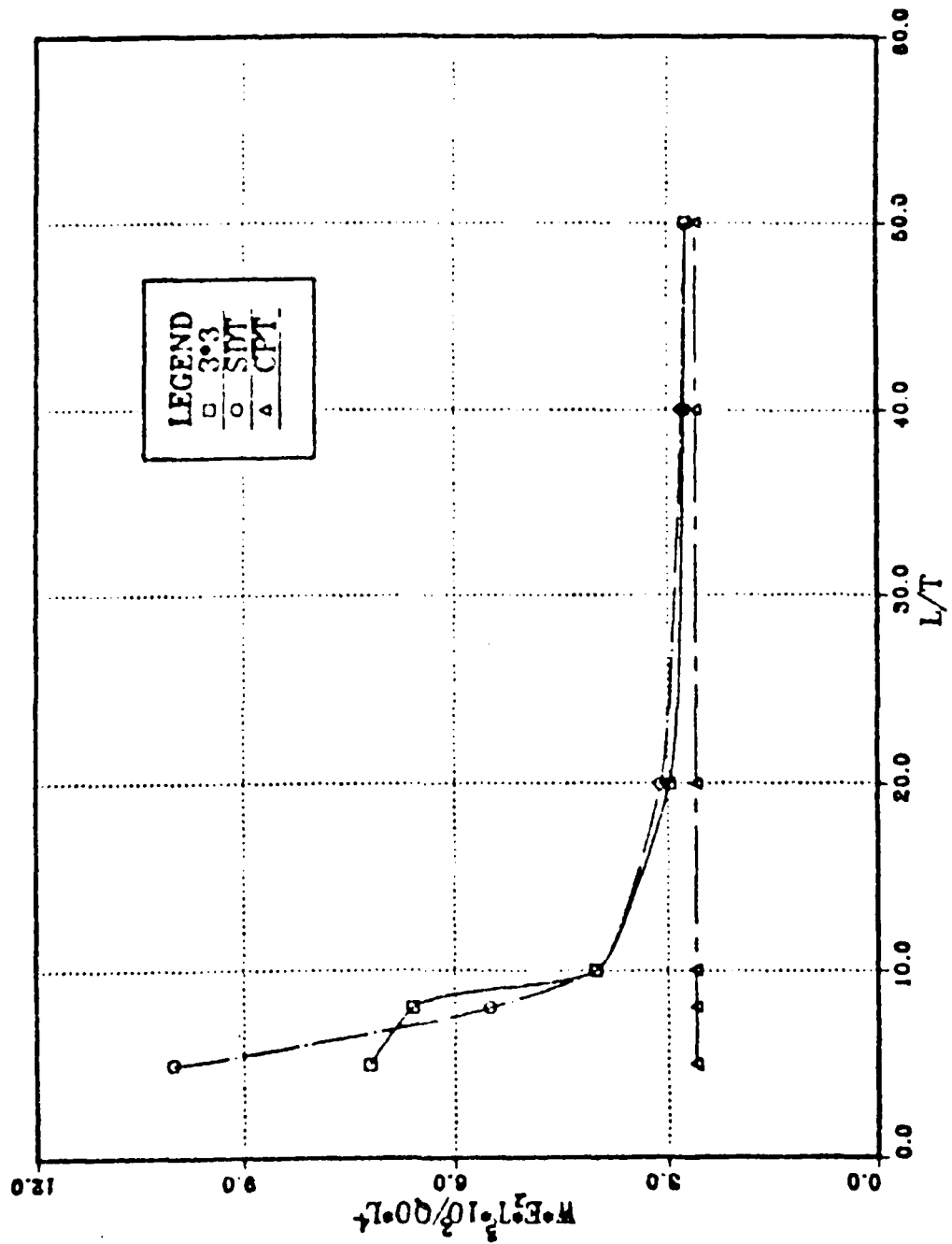


Figure 4.12: Central Deflection W_{max} of 4-Layered Square Plate
(Case I: Graphite-Epoxy)

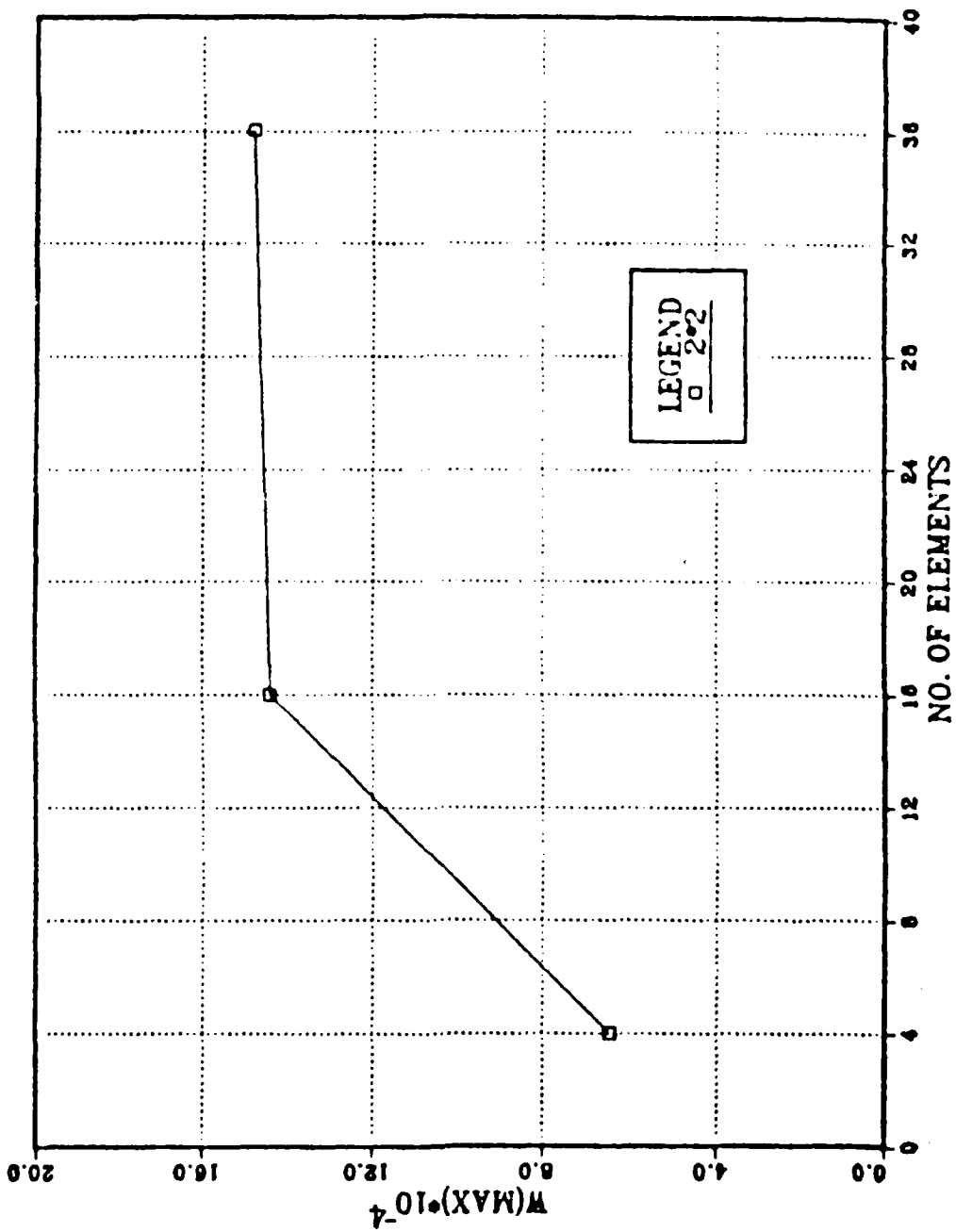


Figure 4.13: W_{max} vs. No. of Elements for 4-Layered Square Plate
 (Case I: Graphite-Epoxy)

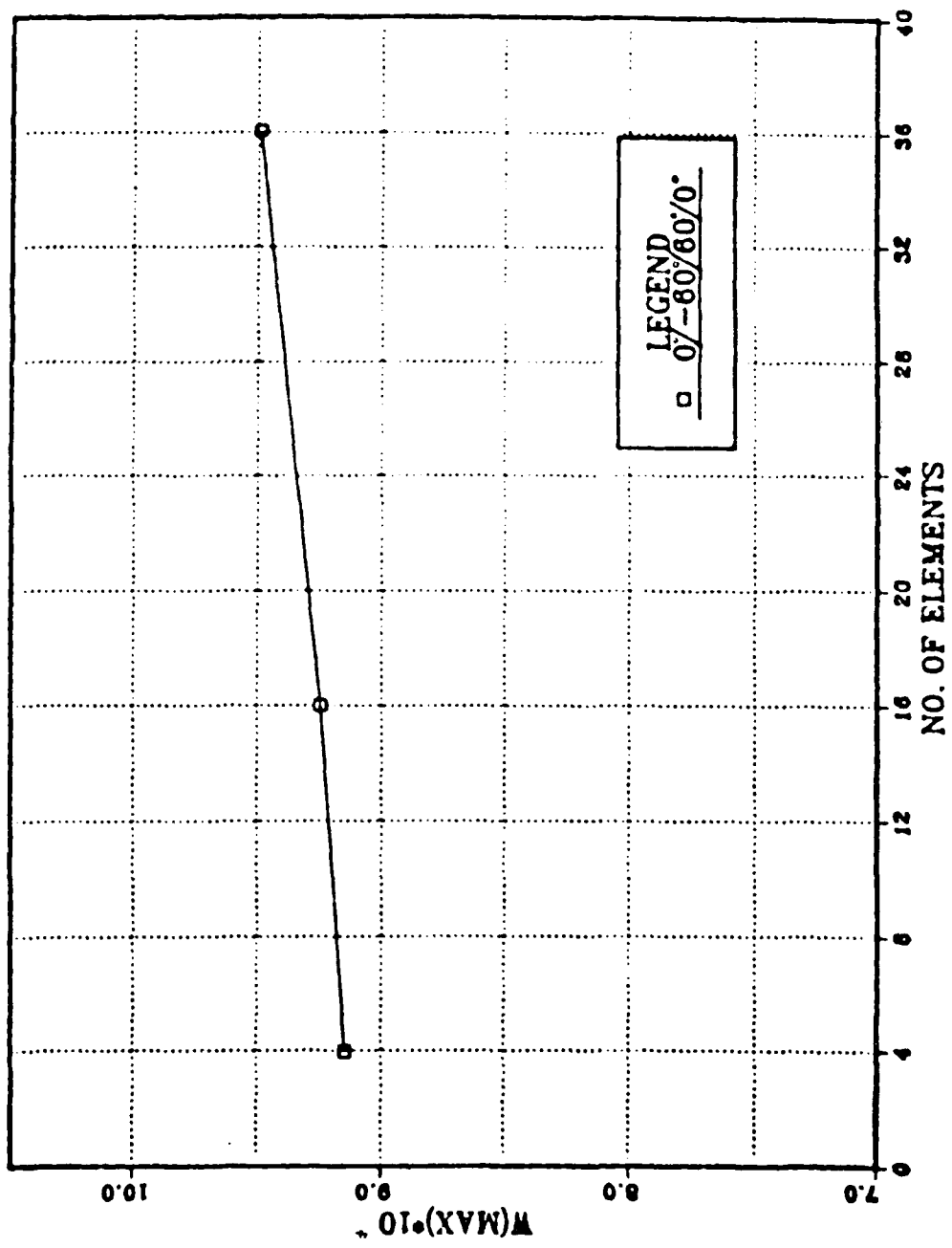


Figure 4.14: W_{max} vs. No. of Elements for 4-Layered Square Plate
(Case II: Graphite-Epoxy)

The plate is subjected to a transverse sinusoidal load of intensity.

$$q = q_0 \sin \frac{\pi x}{L} \sin \frac{\pi y}{L} \quad (4.14)$$

Figure 4.15 shows the maximum deflection of this element and of shear deformation theory [Ref. 24] and elasticity solution [Refs. 16, 17, 18] for analytical solution. Good agreement is obtained for thin plates while discrepancies exist for thick plates. Convergence characteristics are shown in Figures 4.16 and 4.17.

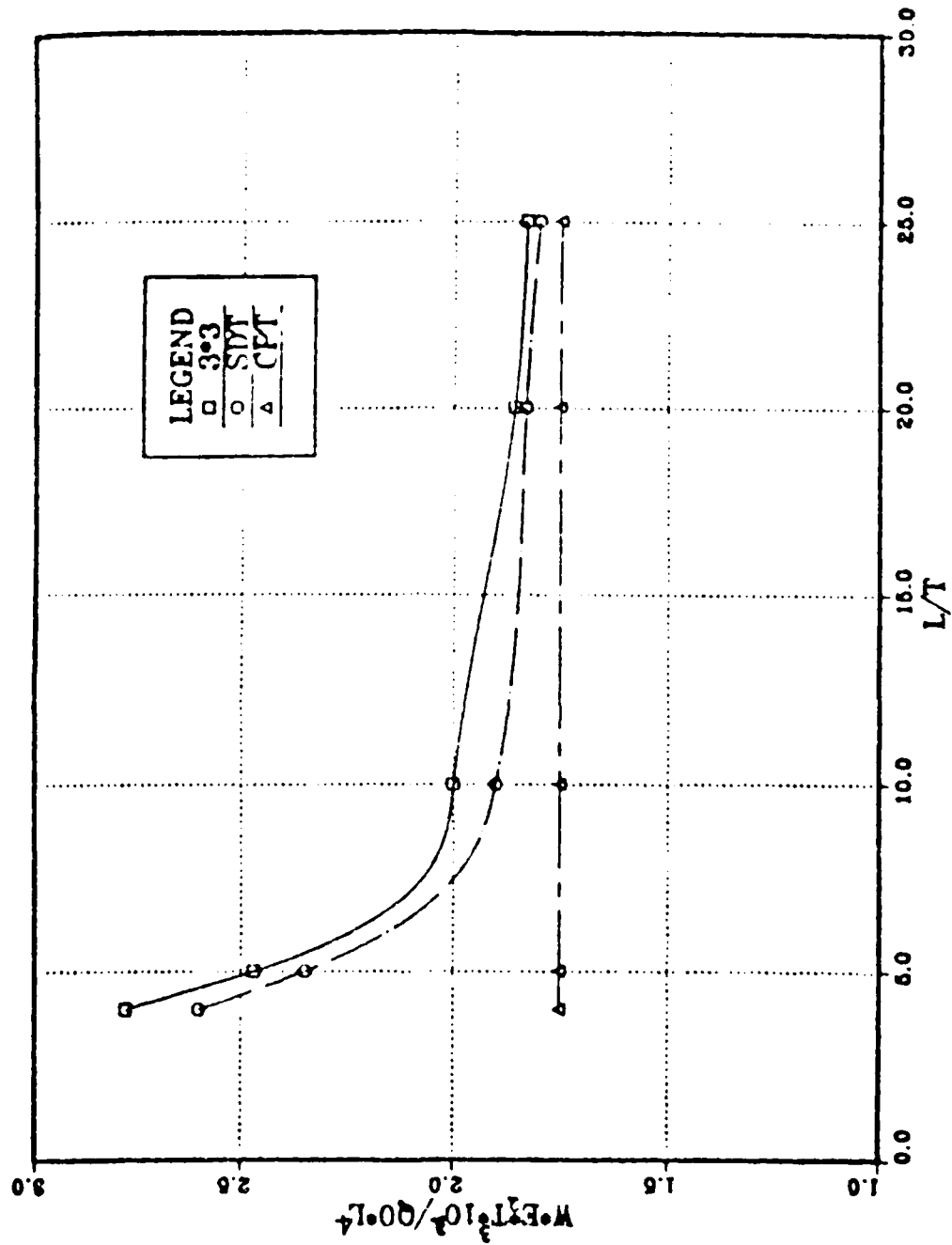


Figure 4.15: Central Deflection W_{max} for 4-Layered Square Plate
(Case III: Glass-Epoxy)

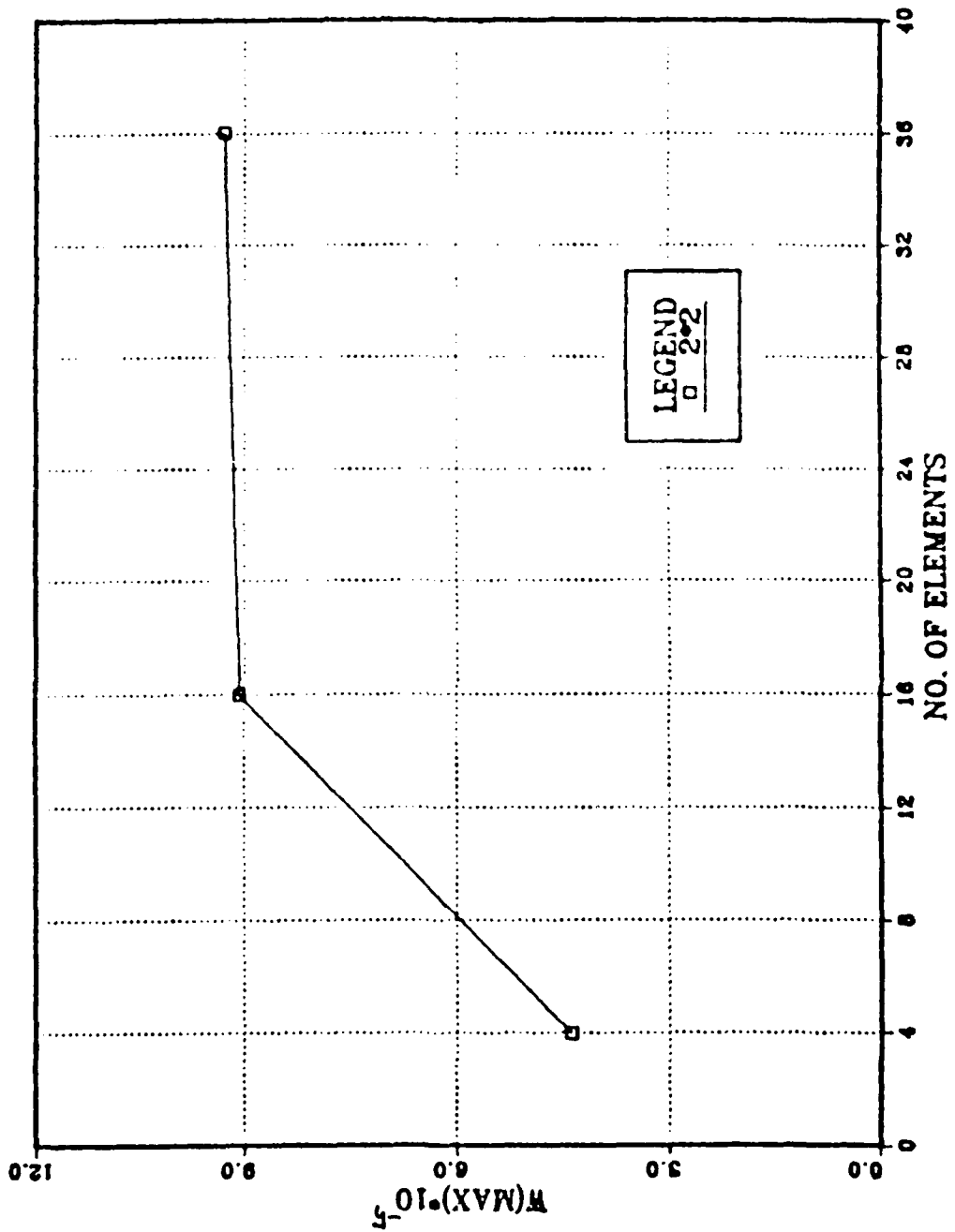


Figure 4.16: W_{max} vs. No. of Elements for 4-Layered Square Plate
(Case III: Glass-Epoxy)

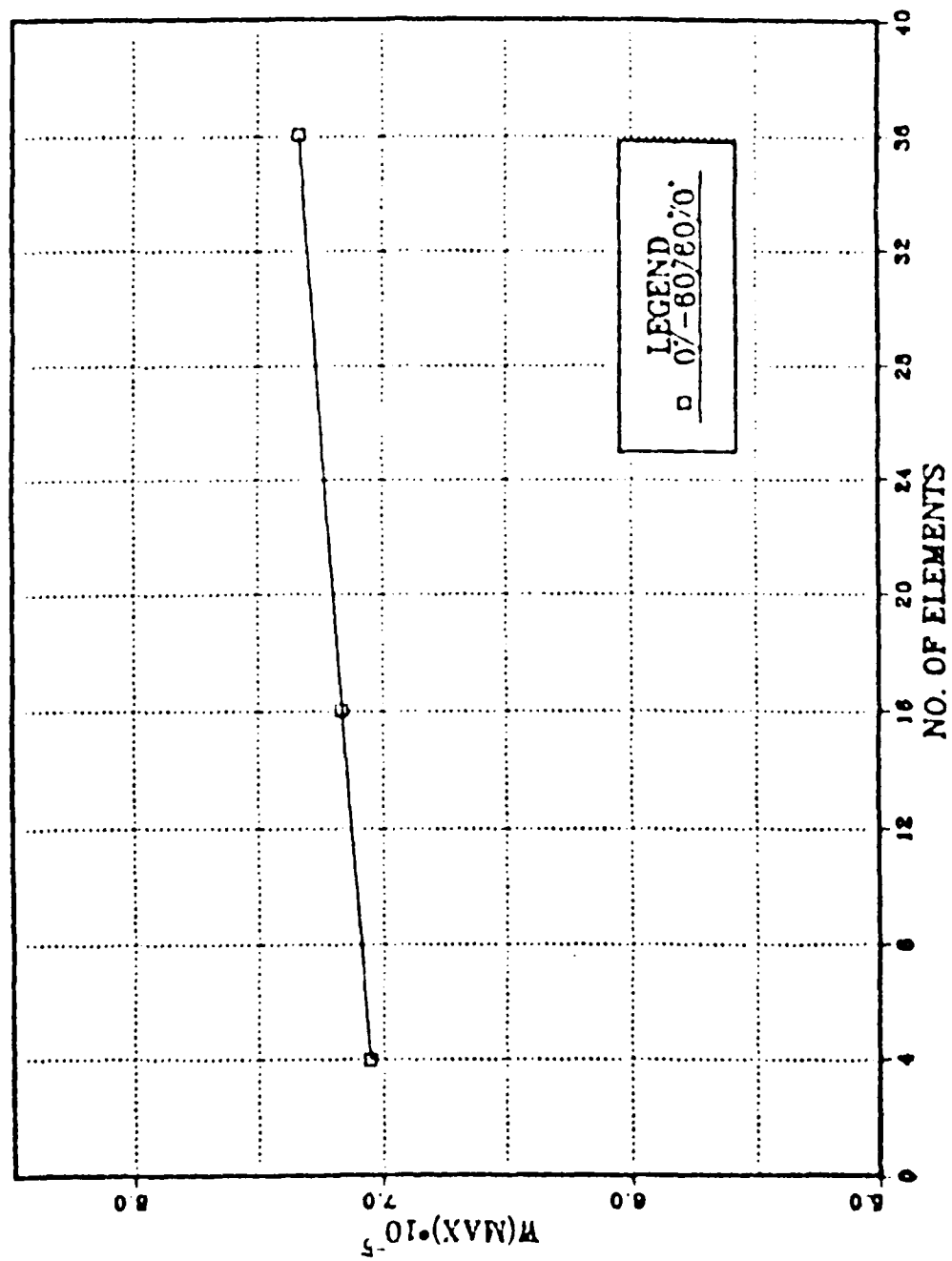


Figure 4.17: W_{max} vs. No. of Elements for 4-Layered Square Plate
(Case IV: Glass-Epoxy)

V. CONCLUSIONS

This study is directed towards understanding the linear static analysis of plates composed of both isotropic and laminated composites.

The formulation is based on the principle of virtual work. A finite element formulation is presented as a model for the analysis of laminated anisotropic plate structures. Several numerical examples for the isotropic elastic plates are solved for different boundary conditions and loadings.

The results show that bi-quadratic isoparametric lagrange plate bending element is effective for analysis of laminated anisotropic plates. Numerical solutions agree well with analytical solution. Further, it is observed that as the number of elements are increased, the convergence to analytical solution is assured.

The element predicts good results for thin plates while large discrepancies exist for thick plates and calls for further investigation. In general, a 3×3 integration seems to predict the solutions well.

More numerical experiments need to be done regarding selective integrations, and apply to a variety of layer configurations for composite plates. Another area is in including the nonlinear terms for buckling problems. The free-vibration analysis to predict the natural frequencies and mode shapes is an obvious extension.

LIST OF REFERENCES

1. Zienkiewicz, O. C., *The Finite Element Method*, 3rd ed., McGraw-Hill Co., 1977.
2. Mindlin, R. D., "Influence of Rotatory Inertia and Shear on Flexural Motions of Isotropic, Elastic Plates," *Journal of Applied Mechanics*, v. 18, pp. 31-38, 1951.
3. Hughes, T. R., Cohen, M. and Maroun, M., "Reduced and selective Integration Techniques in the Finite Element Analysis of Plates," *Nuclear Engineering and Design*, v.46, pp. 203-222, 1978.
4. Hughes, T.R. and Cohen, M., "The Heterosis Finite Element for Plate Bending," *Computers and Structures*, v. 9, pp. 445-450, 1978.
5. Reissner, E. and Stavsky, Y., "Bending and Stretching of Certain Types of Heterogeneous Anisotropic Elastic Plates," *Journal of Applied Mechanics*, v. 28, pp. 402-408, 1961.
6. Whitney, J. M. and Leissa, A. W., "Analysis of Heterogeneous Anisotropic Plates," *Journal of Applied Mechanics*, v. 36, pp. 262-266, 1969.
7. Zienkiewicz, O. C., Taylor, R. L. and Loo, J. M., "Reduced Integration Technique in General Analysis of Plates and Shells," *International Journal for Numerical Methods in Engineering*, v. 3, pp. 575-586, 1971.
8. Pryor, C. W. and Barker, R. M., "A Finite Element Analysis Including Transverse Shear Effects for Applications to Laminate Plates," *AIAA Journal*, v. 9, pp. 912-917, 1971.
9. Mawenya, A. W., "Finite Element Analysis of Sandwich Plate Structures," Ph.D. Thesis, University of Wales, Swansea, 1973.
10. Mawenya, A. S. and Davis, J. D., "Finite Element Bending Analysis of Multilayer Plates," *International Journal for Numerical Methods in Engineering*, v. 8, pp. 215-225, 1974.
11. Krishna Murty, A. V., "Flexure of Composite Plates," *Composite Structures*, v. 7, pp. 161-177, 1987.
12. Lo, K. H., Christensen, R. M. and Wu, E. M., "A Higher Order Theory of Plate Deformation, Part I: Homogeneous Plates," *Journal of Applied Mechanics*, v. 44, pp. 662-668, 1977.
13. Lo, K. H., Christensen, R. M. and Wu, E. M., "A Higher Order Theory of Plate Deformation, Part II: Laminated Plates," *Journal of Applied Mechanics*, v. 44, pp. 669-676, 1977.
14. Bert, C. W., "Critical Evaluation of New Plate Theories Applied to Laminated Composites," *Composite Structures*, v. 2, pp. 329-347, 1984.

15. Srinivas, S. and Rao, A. K., "Bending, Vibration and Buckling of Simply Supported Thick Orthotropic Rectangular Plates and Laminates," *International Journal of Solids and Structures*, v. 6, pp. 1463-1481, 1970.
16. Pagano, N. J., "Exact Solution for Rectangular Bidirectional Composites and Sandwich Plates," *Journal of Composite Materials*, v. 4, pp. 20-34, 1970.
17. Pagano, N. J., "Influence of Shear Coupling in Cylindrical Bending of Anisotropic Plates," *Journal of Composite Materials*, v. 4, pp. 330-343, 1970.
18. Pagano, N. J. and Hatfield, S. J., "Elastic Behavior of Multilayered Bidirectional Composites," *AIAA Journal*, v. 10, pp. 931-933, 1972.
19. Pagano, N. J., "Exact Solutions for Composite Laminates in Cylindrical Bending," *Journal of Composite Materials*, v. 3, pp. 398-411, 1969.
20. Srinivas, S. and Rao, A. K., "Bending, Vibration and Buckling of Simply Supported Thick Orthotropic Rectangular Plates and Laminates," *International Journal of Solids and Structures*, v. 6., pp. 1463-1481, 1970.
21. Vinson, J. R. and Chou, T. W. *Composite Materials and Their Use in Structures*, Applied Science Publishers, London, 1975.
22. El Naschie, M. S., "Initial and Post Buckling of Axially Compressed Orthotropic Cylindrical Shells," *AIAA Journal*, v. 14, pp. 1502-1504, Oct. 1976.
23. NASA Technical Report R-402, *Analysis of Laminated Composite Circular Cylindrical Shells with General Boundary Conditions*, by Srinivas, S., p. 76, Apr. 1974.
24. Whitney, J. M., "The Effect of Transverse Deformation on the Bending of Laminated Plates," *Journal of Composite Materials*, v. 3, pp. 134-147, 1969.
25. Mau, S. T., "A Refined Laminated Plate Theory," *Journal of Applied Mechanics*, v. 40, p. 606, 1973.
26. Yang, P. C., Norris, C. H. and Stavsky, Y., "Elastic Wave Propagation in Heterogeneous Plates," *International Journal of Solids and Structures*, v. 2, pp. 665-804, 1966.
27. Reddy, J. N., "Simple Higher Order Theory for Laminated Composite Plate," *Journal of Applied Mechanics*, v. 51, pp. 745-752, 1984.
28. Reddy, J. N. and Sandidge, D. *Mixed Finite Element Models for Laminated Composite Plates*, paper presented at the Winter Annual Meeting of the American Society of Mechanical Engineers, Miami Beach, Fl, 17 Nov. 1985.
29. Gorji, M., "On Large Deflection of Symmetric Composite Plates Under Static Loading," *Journal of Mechanical Engineering Science*, v. 200, pp. 13-19, 1986.
30. Hearman, R. F. S., *An Introduction to Applied Anisotropic Elasticity*, Oxford University Press, 1961.
31. Lekhnitskii, S. G., *Theory of Elasticity of an Anisotropic Elastic Body*, Hoden-Day Inc., 1963.

32. Tsai, S. W., "Mechanics of Composite Material," Part II, Technical Report AFML-TR-66-149, Nov. 1966.
33. Tsai, S. W. and Pagano, N. J., "Invariant Properties of Composite Materials," *Composite Materials Workshop*, Technomic Publishing Co., January, 1968.
34. Gibert, R. P. and Schneider, M., "Linear Anisotropic Plate," *Journal of Composite Materials*, v. 15, pp. 71-78, 1981.
35. Noor, A. K. and Mathers, M. D., "Anisotropy and Shear Deformation in Laminated Composite Plates," *AIAA Journal*, v. 14, p. 282-285, 1976.
36. Noor, A. K. and Mathers, M. D., "Finite Element Analysis of Anisotropic Plates," *International Journal for Numerical Methods in Engineering*, v. 11, pp. 289-307, 1977.
37. Hinton, E., "The Flexural Analysis of Laminated Composites Using A Parabolic Isometric Plate Bending Element," *International Journal for Numerical Methods in Engineering*, v. 11, pp. 174-179, 1977.
38. Bathe, K. J., *Finite Element Procedures in Engineering Analysis*, Prentice-Hall, Inc., 1982.
39. Weaver, W. Jr. and Johnston, P. R., *Finite Elements for Structural Analysis*, Prentice-Hall, Inc., 1984.
40. Nelson, R. B. and Lorch, D. R., "Refined Theory for Laminated Orthotropic Plates," *American Society of Mechanical Engineers*, n. 73-APM-KKK, p. 7, 1973.

INITIAL DISTRIBUTION LIST

	No. of Copies
1. Defense Technical Information Center Cameron Station Alexandria, Virginia 22304-6145	2
2. Library, Code 0142 Naval Postgraduate School Monterey, California 93943-5002	2
3. Superintendent Naval Postgraduate School Attn: Chairman, Department of Aeronautics and Astronautics Code 67 Monterey, California 93943-5000	1
4. Superintendent Naval Postgraduate School Attn: Professor Ramesh Kolar Code 67Kj Monterey, California 93943	4
5. Personnel Management Office Air Force Headquarters Sindaebang Dong, Kwanak Gu, Seoul, Republic of Korea	2
6. Air Force Central Libray Chongwon Gun, Chungcheong Bug Do, Republic of Korea	2
7. 3rd Department of Air Force College Chungwon Gun, Chungcheong Bug Do, Republic of Korea	2

8. Library of Air Force Academy 2
Chongwon Gun, Chungcheong Bug Do,
Republic of Korea
9. Lee, Myung-Ha 2
214-300, Sangdo 4 Dong,
Dongjak Ku
Seoul, Korea
10. Kee, Ye-Ho 2
SMC 1733
Naval Postgraduate School
Monterey, California 93943
11. Superintendent 1
Naval Postgraduate School
Attn: Professor Gilles Cantin
Code 69
Monterey, California 93943
12. Dr. Rem Jones 1
Code 1823
David Taylor Ship Research Center
Bethesda, Maryland 20084
13. Dr. Anthony K. Amos 1
Program Manager, Aerospace Sciences
AFOSR, Bolling AFB
Washington, D.C. 20332